A G protein–coupled receptor and the intracellular synthase of its agonist functionally cooperate

Chantal Binda,[1,3] Samuel Génier,[1,3] Andréane Cartier,[1,3] Jean-François Larrivée,[2,3] Jana Stankova,[2,3] Jason C. Young,[4] and Jean-Luc Parent[1,3]

[1]Service de Rhumatologie, Département de Médecine, [2]Programme d'Immunologie, Département de Pédiatrie, Faculté de Médecine et des Sciences de la Santé, and [3]Institut de Pharmacologie de Sherbrooke, Université de Sherbrooke, Sherbrooke, Québec, Canada J1H 5N4
[4]Department of Biochemistry, McGill University, Montreal, Québec, Canada, H3G 0B1

Export of newly synthesized G protein–coupled receptors (GPCRs) remains poorly characterized. We show in this paper that lipocalin-type prostaglandin D_2 (PGD_2) synthase (L-PGDS) interacts intracellularly with the GPCR DP1 in an agonist-independent manner. L-PGDS promotes cell surface expression of DP1, but not of other GPCRs, in HEK293 and HeLa cells, independent of L-PGDS enzyme activity. In addition, formation of a DP1–Hsp90 complex necessary for DP1 export to the cell surface is dependent on the interaction between L-PGDS and the C-terminal MEEVD residues of Hsp90. Surprisingly, PGD_2 synthesis by L-PGDS is promoted by coexpression of DP1, suggesting a possible intracrine/autocrine signaling mechanism. In this regard, L-PGDS increases the formation of a DP1–ERK1/2 complex and increases DP1-mediated ERK1/2 signaling. Our findings define a novel cooperative mechanism in which a GPCR (DP1) promotes the activity of the enzyme (L-PGDS) that produces its agonist (PGD_2) and in which this enzyme in turn acts as a cofactor (of Hsp90) to promote export and agonist-dependent activity of the receptor.

Introduction

Prostaglandins (PGs) are lipid autacoids generated from arachidonic acid by the action of cyclooxygenases that produce PGH_2, which is further metabolized by specific synthases to produce PGs, such as PGD_2 (Hirata and Narumiya, 2012). There are two types of PGD_2 synthases. The glutathione-dependent hematopoietic PGD_2 synthase (H-PGDS) is mostly expressed in mast cells (Urade et al., 1990), megakaryocytes (Fujimori et al., 2000), and T-helper 2 lymphocytes (Tanaka et al., 2000), whereas the lipocalin-type PGD_2 synthase (L-PGDS) is glutathione independent and abundantly expressed in the central nervous system, the heart, the retina, and the genital organs (Urade and Hayaishi, 2000).

PGD_2 produces its actions through the activation of two different types of G protein–coupled receptors (GPCRs), the D prostanoid receptor (DP1) and the chemoattractant receptor-homologous molecule expressed on Th2 cells (CRTH2, also known as DP2). Signaling through DP1 causes inhibition of platelet aggregation, bronchodilation, and vasodilation and inhibition of apoptosis of eosinophils, migration, and degranulation of basophils (Chiba et al., 2011) as well as inhibition of bone resorbing activity (Durand et al., 2008).

GPCRs are among the most abundant membrane proteins in humans. They respond to a plethora of ligands to transmit their extracellular signals inside the cell (Lebon and Tate, 2012). They are synthesized in the ER and are then transported to the cell surface where they are typically activated (Conn et al., 2007). Along their life cycle, GPCRs are accompanied by a range of specialized GPCR-interacting proteins to assist nascent receptors in proper folding, to target them to the appropriate subcellular compartments, and to fulfill their signaling tasks (Magalhaes et al., 2012). Dysregulation of GPCR folding, trafficking, and signaling contributes to many pathophysiological processes (Belmonte and Blaxall, 2011; Ulloa-Aguirre and Michael Conn, 2011; Vassart and Costagliola, 2011; Lappano and Maggiolini, 2012). However, the specific molecular mechanisms underlying these pathways for GPCRs are still largely unknown.

Correspondence to Jean-Luc Parent: jean-luc.parent@usherbrooke.ca

Abbreviations used in this paper: EIA, enzyme immunoassay; GPCR, G protein–coupled receptor; H-PGDS, hematopoietic PGD_2 synthase; L-PGDS, lipocalin-type PGD_2 synthase; PDI, protein disulfide isomerase; PG, prostaglandin; TPR, tetratricopeptide repeat.

The Rockefeller University Press $30.00
J. Cell Biol. Vol. 204 No. 3 377–393
www.jcb.org/cgi/doi/10.1083/jcb.201304015

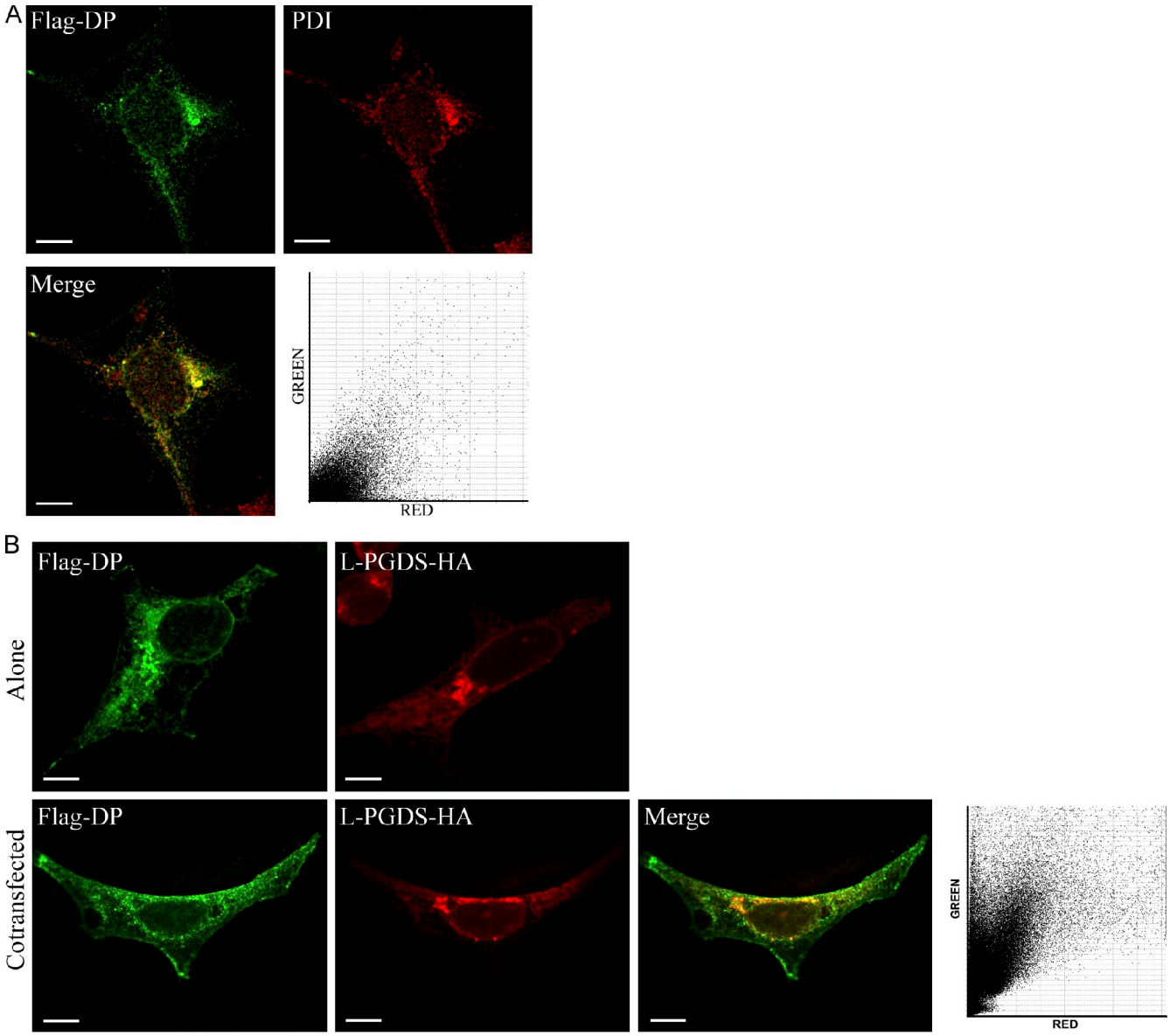

Figure 1. **L-PGDS colocalizes intracellularly with DP1.** (A) HEK293 cells were transiently transfected with a pcDNA3-Flag-DP1 construct for 48 h. The cells were fixed and prepared for confocal microscopy as described under Materials and methods. DP1 was visualized using Flag-specific monoclonal and Alexa Fluor 488–conjugated anti–mouse IgG antibodies (green). Endogenous PDI was detected using a PDI-specific polyclonal antibody and Alexa Fluor 546–conjugated anti–rabbit IgG (red). An overlay of staining patterns of green-labeled DP1 and red-labeled PDI (merge) and the corresponding fluorogram are shown. (B) HEK293 cells were transiently transfected with pcDNA3-Flag-DP1, pcDNA3–L-PGDS–HA, or both for 48 h. The cells were then fixed and prepared for confocal microscopy as in A. L-PGDS was visualized using HA-specific monoclonal and Alexa Fluor 633–conjugated anti–mouse IgG antibodies (red). DP1 was visualized using a Flag-specific polyclonal and Alexa Fluor 488–conjugated anti–rabbit IgG antibodies (green). An overlay of staining patterns of the green-labeled DP1 and red-labeled L-PGDS (merge) and the corresponding fluorogram are shown. Bars, 10 µM.

Molecular chaperones mediate the correct assembly and folding of polypeptides or set off reactions that lead to degradation of misfolded proteins (Imai et al., 2003; Kriegenburg et al., 2012; Rodrigo-Brenni and Hegde, 2012; Wang et al., 2013). Among the conserved chaperones are the heat shock proteins that are activated in response to heat, nutrient deprivation, oxidative stress, and other conditions that threaten cell survival (Hartl et al., 2011). Hsp90 is a major, ubiquitous cytoplasmic chaperone that plays a crucial role in folding, assembly, and stabilization of cytosolic and membrane proteins, in addition to facilitating protein complex assembly and intracellular cell signaling (Zhao and Houry, 2007; Gorska et al., 2012; Jackson, 2013; Zuiderweg et al., 2013). Hsp90 is aided in its functions by a variety of co-chaperones, which associate with Hsp90 to modulate its chaperoning activity and/or recruit it to specific substrates. Hsp90 has been proposed to be involved in the regulation of vesicular trafficking (Sakisaka et al., 2002; Chen and Balch, 2006; McClellan et al., 2007; Taipale et al., 2010).

Our previous studies have shown that a large population of DP1 is retained in intracellular compartments after synthesis (Parent et al., 2010; Labrecque et al., 2013). Furthermore, we reported that L-PGDS was localized to the ER and other intracellular compartments (Mathurin et al., 2011). Given the fact

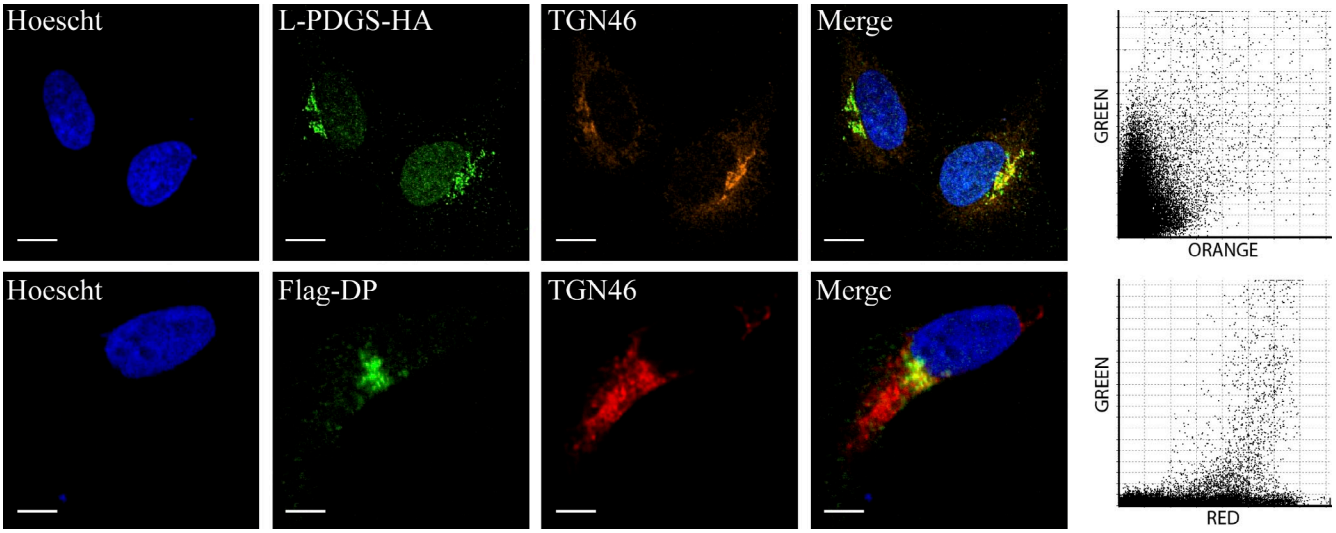

Figure 2. **Both L-PGDS and DP1 localize to the TGN.** HEK293 cells were transiently transfected with pcDNA3-Flag-DP1 or pcDNA3–L-PGDS–HA for 48 h. The cells were then fixed and prepared for confocal microscopy as described under Materials and methods. L-PGDS was visualized using HA-specific monoclonal and Alexa Fluor 546–conjugated anti–mouse IgG antibodies (orange). DP1 was visualized using Flag-specific polyclonal and Alexa Fluor 633–conjugated anti–mouse IgG antibodies (red). Endogenous TGN was detected using a TGN46-specific polyclonal antibody and Alexa Fluor 488–conjugated anti–rabbit IgG (green). An overlay of staining patterns of the green-labeled TGN46 and orange-labeled L-PGDS or red-labeled DP1 (merge) and the corresponding fluorogram are shown. Bars, 10 µM.

that both proteins have similar intracellular distribution, our interest was to investigate whether L-PGDS could interact with DP1 and have an effect on its trafficking and function. We report that DP1 and L-PGDS exert mutual regulation on PGD_2 production by L-PGDS and on DP1 export and signaling.

Results

Intracellular colocalization between L-PGDS and DP1

The first experiment conducted was to confirm the localization of DP1 at the ER. Confocal microscopy revealed colocalization between Flag-DP1 and protein disulfide isomerase (PDI) at the ER in HEK293 cells (Fig. 1 A). We had showed before that L-PGDS was localized at the nucleus, the cytoplasm, the ER, and other intracellular compartments (Mathurin et al., 2011). The possible colocalization between L-PGDS–HA and Flag-DP1 was thus examined in HEK293 cells to reveal that both proteins displayed a predominant association with vesicular structures in the cytoplasm with an increased concentration within the perinuclear region (Fig. 1 B, top). Colocalization between L-PGDS and DP1 was not observed at the plasma membrane. Furthermore, coexpression of L-PGDS appeared to increase the cell surface expression of DP1, which can be seen as a more defined cell outline compared with DP1 staining in the single-transfected cells (Fig. 1 B, bottom). This result suggests that the presence of L-PGDS promotes the cell surface expression of DP1.

We then wanted to assess whether L-PGDS and DP1 could also be found in the TGN, further in the maturation route of the receptor. Localization of DP1 and L-PGDS was then compared to that of a TGN marker, TGN46. Fig. 2 shows that both L-PGDS and DP1 colocalized with TGN46 in the perinuclear region in HEK293 cells.

L-PGDS interacts with DP1

Because L-PGDS and DP1 colocalized intracellularly, we wanted to assess whether there was an interaction between the two proteins and whether this interaction could be direct. We performed in vitro binding assays using purified DP1 intracellular domains in fusion with GST along with purified L-PGDS fused to a hexahistidine tag (His–L-PGDS). As shown in Fig. 3 A, L-PGDS interacted with GST-DP1–carboxyl terminus and GST-DP1-ICL2 but not with GST alone, GST-DP1-ICL1, and GST-DP1-ICL3.

To study the interaction in a cellular context, we performed immunoprecipitation assays on lysates of HEK293 cells transiently transfected with Flag-DP1 and L-PGDS–HA with a Flag-specific monoclonal antibody. Coimmunoprecipitation of L-PGDS with DP1 was detected by Western blot analysis with a HA antibody (Fig. 3 B). Stimulation of the receptor with PGD_2 did not modulate the quantity of L-PGDS that coimmunoprecipitated with DP1. Coexpression of the two proteins and receptor stimulation did not alter the total expression of DP1 or L-PGDS. The DP1–L-PGDS interaction could be detected at the endogenous level from lysates of HT-29 human colon adenocarcinoma cells, which express detectable levels of both endogenous proteins (Fig. 3 C). Altogether, our results show that the interaction between L-PGDS and DP1 occurs in the perinuclear region, can be direct, takes place at the endogenous level, and is not modulated by DP1 stimulation.

Specific regulation of DP1 export by L-PGDS

Following the results obtained by confocal microscopy, our next interest was to verify whether L-PGDS could promote the cell surface expression of DP1, although the total expression of the receptor remained unchanged. Cell surface expression assays were performed by ELISA in HEK293 cells, as we described previously (Parent et al., 2009, 2010; Cartier et al., 2011; Lachance

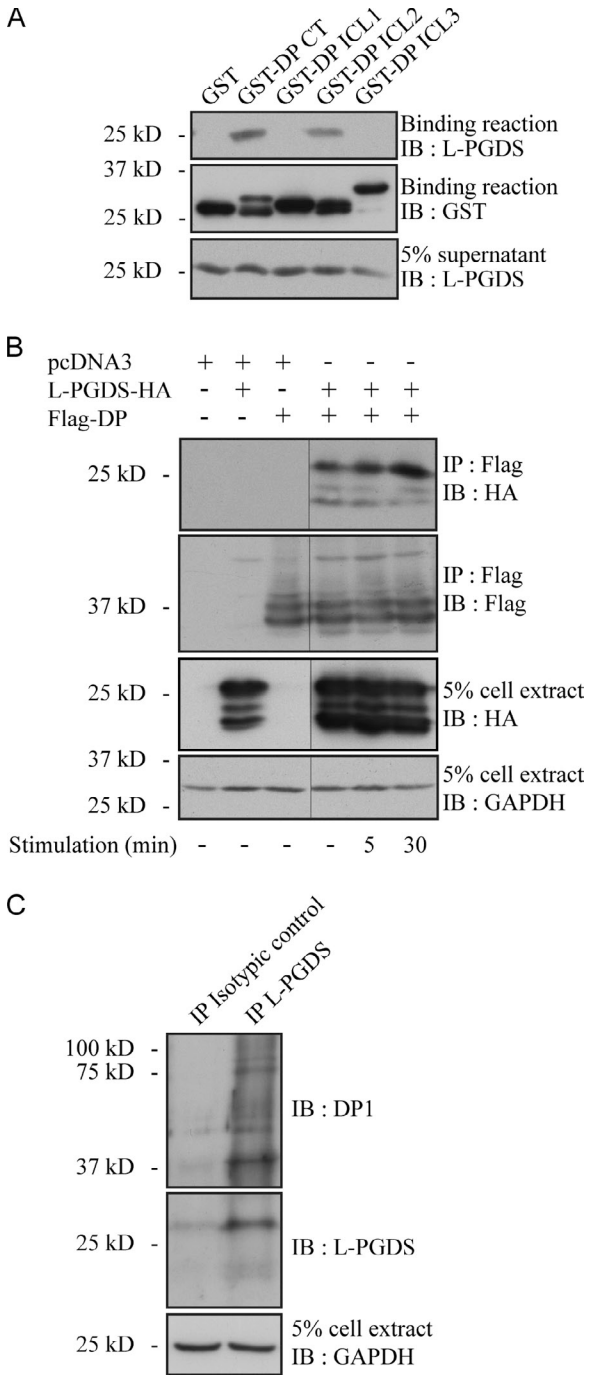

Figure 3. **L-PGDS interacts with DP1.** (A) Binding assays were performed using purified glutathione-Sepharose–bound GST-DP1–carboxyl terminal (CT) and intracellular loops (ICL) incubated with purified His_6–L-PGDS. The binding of L-PGDS to the receptor domains was detected by immunoblotting (IB) using an L-PGDS–specific polyclonal antibody, and the GST fusion proteins present in the binding reaction were detected using an anti-GST antibody. Blots shown were spliced but came from the same gels. (B) HEK293 cells transiently transfected with Flag-DP1 and L-PGDS–HA were stimulated or not stimulated with 1 µM PGD_2 for 5 or 30 min. Immunoprecipitation (IP) of the receptor was performed using a Flag-specific monoclonal antibody, and immunoblotting was performed with Flag-specific polyclonal or peroxidase-conjugated anti-HA antibodies. Black lines indicate that intervening lanes have been spliced out. (C) Immunoprecipitation was performed in HT-29 cells using L-PGDS–specific monoclonal or rat isotypic control IgG antibodies, and immunoblotting was performed using L-PGDS–specific polyclonal or DP1-specific polyclonal antibodies. Blots shown are representative of three independent experiments.

et al., 2011; Mathurin et al., 2011). Coexpression of L-PGDS significantly increased the cell surface expression of DP1, in contrast to coexpression of H-PGDS (Fig. 4 A). Parallel experiments were conducted to verify whether L-PGDS could also act similarly on CRTH2 (the other PGD_2 receptor) and other GPCRs, such as the β_2-adrenergic receptor, thromboxane A_2 receptor (TP-α), angiotensin II type I receptor, and the wild-type arginine vasopressin receptor 2 and its intracellularly trapped W164S and Y205C mutants (Oksche et al., 1996). Coexpression of L-PGDS had no effect on cell surface expression of the other GPCRs (Fig. 4 A). Collectively, these results demonstrate that, among the GPCRs that were tested, the effect of L-PGDS on potentiating receptor cell export is specific to DP1, which was reflected in its specificity for interacting with DP1 (Fig. S1).

Because HEK293 cells do not express detectable levels of endogenous L-PGDS, the role of the endogenous synthase was studied in HeLa cells stably expressing HA-DP1 transfected with control or L-PGDS siRNAs. HeLa cells were chosen because they express both L-PGDS and DP1 at endogenous levels, although at lower levels than HT-29 cells, but can easily be transfected. Efficiency of L-PGDS depletion by the siRNAs was evaluated by Western blot analysis (Fig. 4 B). Corroborating our overexpression experiments, cell surface expression of DP1 was significantly reduced when L-PGDS was depleted (Fig. 4 C).

Given the modulation of DP1 cell surface expression, we wanted to study the effect of L-PGDS on the internalization of DP1. Internalization experiments revealed no difference between the agonist-induced internalization of the receptor alone or in the presence of L-PGDS (Fig. 4 D). Thus, L-PGDS increased the cell surface expression of DP1 while having no effect on its internalization. We also studied the PGD_2 production through L-PGDS in the presence of the two PGD_2 receptors. Surprisingly, the assays revealed an increase in PGD_2 production when L-PGDS was cotransfected with DP1 in HEK293 cells but not with CRTH2 (Fig. 4 E). To our knowledge, this is the first demonstration of a GPCR modulating the activity of the enzyme that produces its agonist.

It could be viewed as counterintuitive that the DP1–L-PGDS interaction, which promotes PGD_2 synthesis results in an increase in DP1 cell surface expression rather than in agonist-induced internalization of the receptor. We conjectured that perhaps the two mechanisms were happening simultaneously but that the effect on DP1 export out balanced that of its agonist-induced internalization. To test our hypothesis, we measured the promotion of cell surface expression of stably expressed Flag-DP1 in HeLa cells by L-PGDS in presence of the specific DP1 antagonist BW868C or of coexpressed dynamin-K44A, a dominant-negative mutant of dynamin that blocks PGD_2-induced internalization of DP1 (Gallant et al., 2007). Our data show that the L-PGDS–mediated increase in DP1 export to the plasma membrane is augmented when agonist-induced internalization of DP1 is blocked by the receptor antagonist or by dynamin-K44A (Fig. 4 F). This supports our idea that, although both mechanisms happen simultaneously, the potential of the DP1–L-PGDS interaction to favor DP1 transport to the cell surface offsets the agonist-induced internalization of DP1 that occurs as a consequence of the increased PGD_2 production, resulting in a net gain of DP1 cell surface expression.

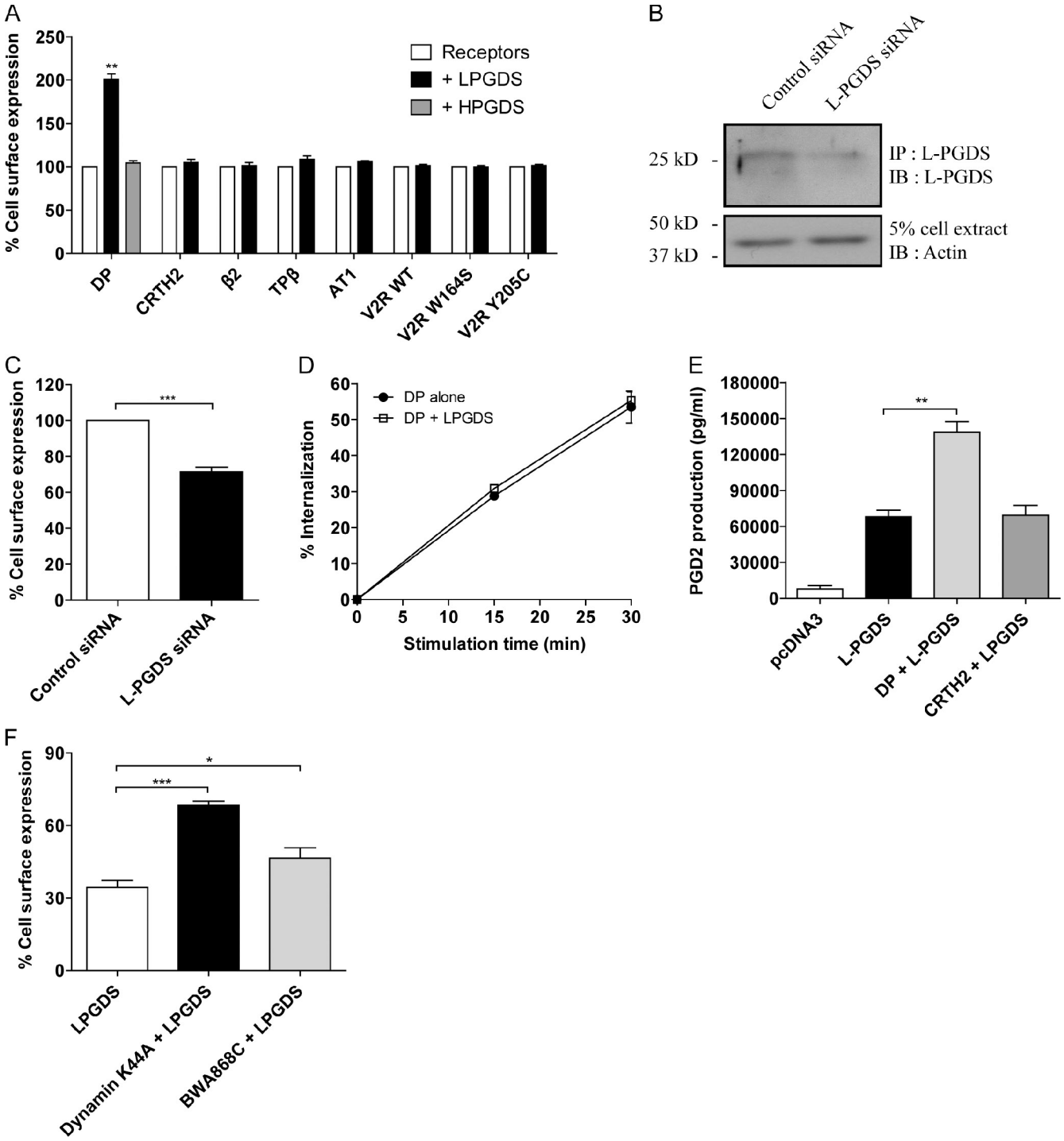

Figure 4. **L-PGDS regulates the cell surface expression of DP1 but not of other tested GPCRs.** (A) Cell surface expression of the receptors was measured by ELISA in cells transiently transfected for 48 h with Flag-tagged receptors in combination with pcDNA3, pcDNA3–L-PGDS–HA, or pcDNA3–H-PGDS–HA. Results are shown as the percentage of cell surface expression of the receptors when cells were transfected with L-PGDS or H-PGDS compared with cell surface expression of the receptors when they were transfected with pcDNA3. (B) HeLa cells were transfected with negative control or L-PGDS siRNAs for 72 h. Immunoprecipitation (IP) of L-PGDS was performed using an L-PGDS–specific monoclonal antibody, and immunoblotting (IB) was performed with an L-PGDS–specific polyclonal antibody. (C) Cell surface expression of stably transfected HA-DP1 was measured by ELISA in HeLa transfected with negative control or L-PGDS siRNAs for 72 h. (D) Agonist-induced internalization of DP1 was studied in HEK293 cells after 15 and 30 min of stimulation with 1 μM PGD_2. (E) HEK293 cells were transiently transfected with the indicated combinations of pcDNA3, Flag-DP1, L-PGDS–HA, or Flag-CRTH2 for 48 h. Cells were then incubated with 5 μM PGH_2 for 15 min. Supernatants were assessed for PGD_2 production by commercial enzyme-linked immunoassays as described under Materials and methods. (F) Cell surface expression of stably expressed Flag-DP1 in HeLa cells transiently transfected with L-PGDS–HA alone, in combination with dynamin-K44A, or treated with BWA868C was measured by ELISA. All values are the means ± SE from at least three separate experiments. *, $P < 0.05$; **, $P < 0.01$; ***, $P < 0.001$.

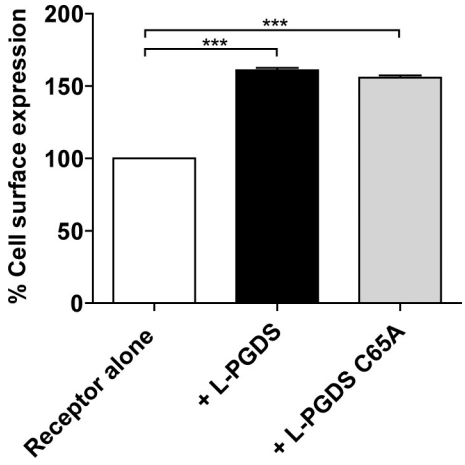

Figure 5. **The enzyme activity of L-PGDS is not required for regulation of DP1 export.** Cell surface expression of DP1 was measured by ELISA in HEK293 cells transiently transfected for 48 h with Flag-DP1 in combination with pcDNA3, pcDNA3–L-PGDS–HA, or pcDNA3–L-PGDS–C65A-HA. Results are shown as the percentage of cell surface expression of DP1 when cells were transfected with L-PGDS or L-PGDS–C65A compared with cell surface expression of DP1 when transfected with pcDNA3. All values are the means ± SE from at least three separate experiments. ***, $P < 0.001$.

The PGD_2 synthase activity of L-PGDS is not required to regulate the export of DP1

To investigate whether the PGD_2 synthase activity of L-PGDS was required for the increase in the export of DP1, we used an L-PGDS–C65A mutant, which is inactive in PGD_2 synthesis (Urade and Hayaishi, 2000; Kumasaka et al., 2009; Zhou et al., 2010). Overexpression of pcDNA3–L-PGDS–HA or pcDNA3–L-PGDS–C65A-HA both resulted in virtually identical increases in cell surface expression of DP1 (Fig. 5), indicating that the PGD_2 synthase activity of L-PGDS is not essential in the promotion of DP1 export.

L-PGDS interacts with Hsp90

In an attempt to elucidate the molecular mechanisms underlying the L-PGDS–induced export of DP1, we turned our attention to potential L-PGDS–interacting partners that could participate in this pathway. Molecular chaperones and co-chaperones involved in GPCR export and stability have garnered increasing interest in our laboratory (Parent et al., 2010; Labrecque et al., 2013; Roy et al., 2013). We noticed in the L-PGDS amino acid sequence the presence of a $^{43}\mathbf{W}(X)_2\mathbf{A}\mathbf{G}(X)_2S(X)_9\mathbf{A}(X)_3M(X)_2\mathbf{S}(X)_3\mathbf{P}^{71}$ motif reminiscent of the conserved consensus sequence (bold residues) $\mathbf{W}(X)_2\mathbf{L}\mathbf{G}(X)_2Y(X)_8\mathbf{A}(X)_3F(X)_2\mathbf{S}(X)_4\mathbf{P}$ found in tetratricopeptide repeats (TPRs) used by some co-chaperones to bind to the C-terminal MEEVD residues of Hsp90 (Sikorski et al., 1990; Scheufler et al., 2000; Brinker et al., 2002; Wu et al., 2004; Cliff et al., 2006; Gazda et al., 2013). Although L-PGDS does not contain TPRs, we nevertheless studied whether L-PGDS could interact with Hsp90 in HEK293 cells transiently transfected with L-PGDS–Myc together with Hsp90-HA or its C-terminal ΔMEEVD mutant. As shown in Fig. 6 A, the interaction between L-PGDS and the Hsp90 ΔMEEVD mutant was greatly diminished compared with the interaction between L-PGDS and full-length Hsp90, suggesting that L-PGDS interacted with the C-terminal MEEVD residues of the molecular chaperone. Coimmunoprecipitation between endogenous L-PGDS and Hsp90 was confirmed in HeLa cells (Fig. 6 B). Similar experiments found no interaction between L-PGDS and Hsc70, suggesting that L-PGDS was not interacting with Hsp90 as a misfolded or partially folded client protein. In vitro binding assays using purified Hsp90 in fusion with a histidine tag (His-Hsp90) along with purified untagged L-PGDS showed that L-PGDS interacted directly with Hsp90.

Even though L-PGDS is structurally unrelated to TPR domains, its interaction with the MEEVD motif suggested a comparable contact site, involving charged and hydrophobic interactions. Structures of L-PGDS show a funnel-shaped β barrel with binding sites for ligands in the interior (Hohwy et al., 2008; Kumasaka et al., 2009; Miyamoto et al., 2010). On the outside of the funnel near the bottom, a surface was identified that had basic residues (Arg42, Lys66, Arg151, Lys156, and Lys160) surrounding a sunken hydrophobic site (Trp43, Tyr44, Ala46, and Gly47) under a C-terminal loop (Fig. 6 D). It was possible that the basic residues interact with the Glu and Asp residues of the MEEVD and the hydrophobic residues interact with the Val or Met. Of these residues in human L-PGDS, Trp43 and the basic residues are well conserved in L-PGDS from other species. However, only Trp43 was absolutely conserved in other lipocalin family proteins, and the basic residues showed only moderate to poor conservation. The interaction with the Hsp90 MEEVD may therefore be unique to L-PGDS. An L-PGDS–W43A/G47A construct was thus generated by site-directed mutagenesis. The interaction between the HA-tagged L-PGDS–W43A/G47A mutant and the endogenous Hsp90 was investigated in HEK293 cells and compared with wild-type L-PGDS–HA. As shown in Fig. 6 E, the interaction between endogenous Hsp90 and the L-PGDS–W43A/G47A mutant was significantly decreased compared with wild-type L-PGDS. Altogether, these results indicate that L-PGDS, via a surface with basic and hydrophobic character, interacts directly with the C-terminal MEEVD of Hsp90. This may constitute a new mode of interaction with Hsp90.

L-PGDS promotes the interaction between Hsp90 and DP1

First, we assessed whether Hsp90 modulated the interaction between L-PGDS and the receptor and whether the Hsp90 C-terminal MEEVD residues participate in the association of the chaperone with DP1. Lysates of cells transfected with the indicated combinations of Flag-DP1, L-PGDS–HA, Hsp90-HA, or its ΔMEEVD mutant were incubated with a Flag-specific monoclonal antibody to immunoprecipitate the receptor. Western blot analysis with an HA antibody revealed that the interaction between L-PGDS and DP1 is not modulated by the overexpression of Hsp90 (Fig. 7 A). In contrast, the coimmunoprecipitation between DP1 and the Hsp90 ΔMEEVD mutant is diminished compared with that between the receptor and full-length Hsp90, suggesting that the C-terminal MEEVD motif of the molecular chaperone is important for forming a complex with the receptor.

Second, we performed immunoprecipitation assays in HEK293 cells transiently transfected with Flag-DP1 together with L-PGDS–HA or L-PGDS–W43A/G47A-HA. As shown in

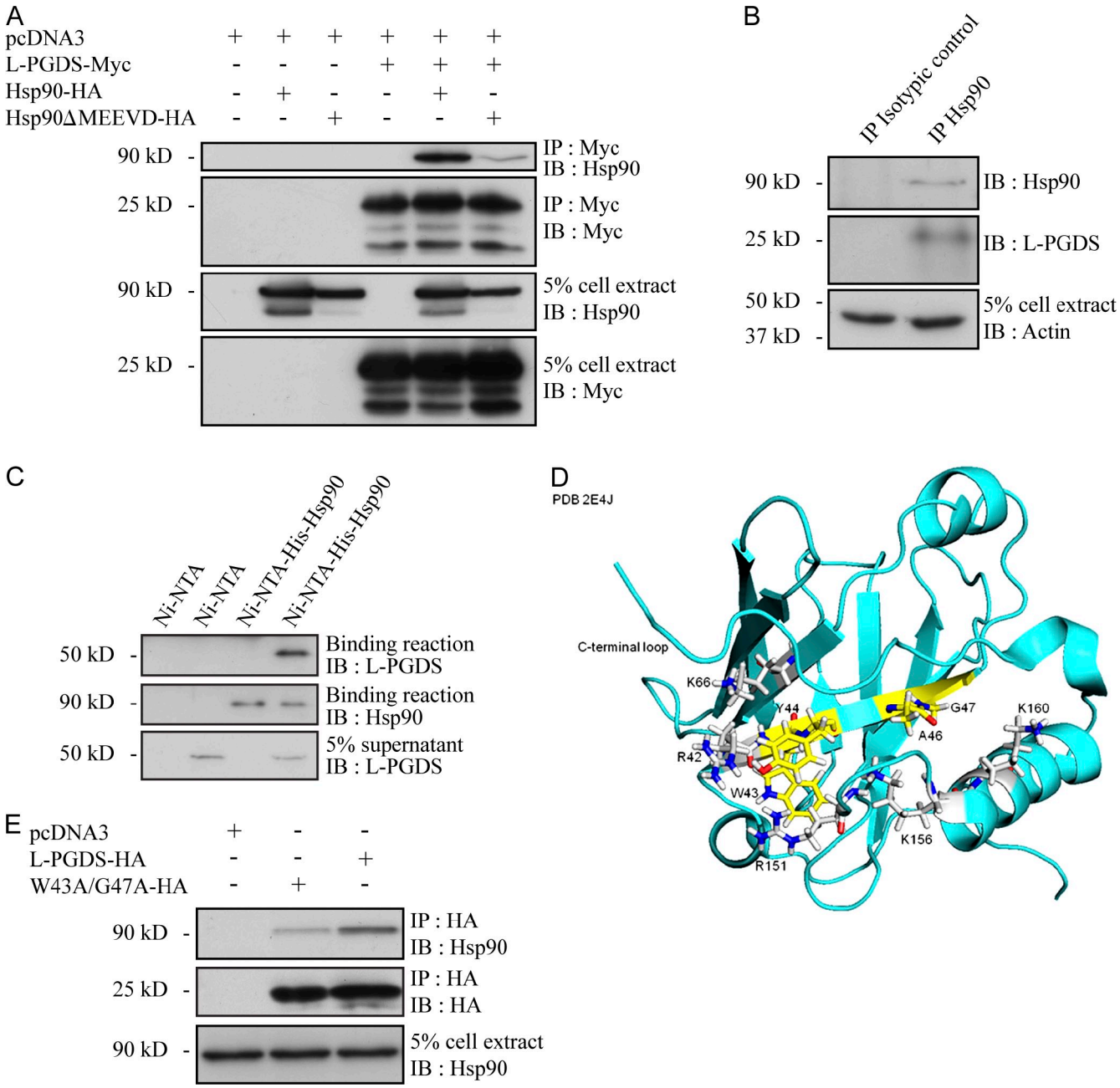

Figure 6. **L-PGDS interacts with Hsp90.** (A) HEK293 cells were transiently transfected with pcDNA3, L-PGDS–Myc, Hsp90-HA, or Hsp90ΔMEEVD-HA mutant constructs. Immunoprecipitation (IP) of L-PGDS was performed using a Myc-specific monoclonal antibody, and immunoblotting (IB) was performed using peroxidase-conjugated anti-Myc or anti-HA antibodies. (B) Immunoprecipitation was performed in HeLa cells using Hsp90-specific monoclonal or mouse isotypic control IgG antibodies, and immunoblotting was performed using Hsp90-specific polyclonal or L-PGDS–specific polyclonal antibodies. (C) His pull-down assays were performed using purified His-Hsp90 bound to Ni^{2+}-agarose beads incubated with purified GST–L-PGDS. The binding of L-PGDS to Hsp90 was detected by immunoblotting using an L-PGDS–specific polyclonal antibody, and the His-Hsp90 present in the binding reaction were detected using an Hsp90-specific polyclonal antibody. (D) Illustration of the funnel-shaped β barrel structure of L-PGDS (available in the Protein Data Bank under accession no. 2E4J). On the outside of the funnel near the bottom, a surface was identified that had basic residues (Arg42, Lys66, Arg151, Lys156, and Lys160) surrounding a sunken hydrophobic site (Trp43, Tyr44, Ala46, and Gly47) under a C-terminal loop. (E) HEK293 cells were transiently transfected with pcDNA3, L-PGDS–HA, or its W43A/G47A-HA mutant construct. Immunoprecipitation of L-PGDS was performed using a HA-specific monoclonal antibody, and immunoblotting was performed using a peroxidase-conjugated anti-HA antibody. Endogenous Hsp90 was detected using an Hsp90-specific polyclonal antibody. Blots shown are representative of three independent experiments. NTA, nitrilotriacetic acid.

Fig. 7 B, coimmunoprecipitation of endogenous Hsp90 with DP1 was detected when L-PGDS was transfected (Fig. 7 B, third lane) but not in the absence of L-PGDS (Fig. 7 B, first lane). In addition, the interaction between Hsp90 and the receptor was much weaker when the L-PGDS–W43A/G47A mutant was expressed (Fig. 7 B, second lane) compared with wild-type L-PGDS (Fig. 7 B, third lane). These data suggest that Hsp90 associates with the receptor through an interaction with L-PGDS because (a) HEK293 cells do not express detectable levels of endogenous L-PGDS and there is no Hsp90 interaction with the receptor in absence of

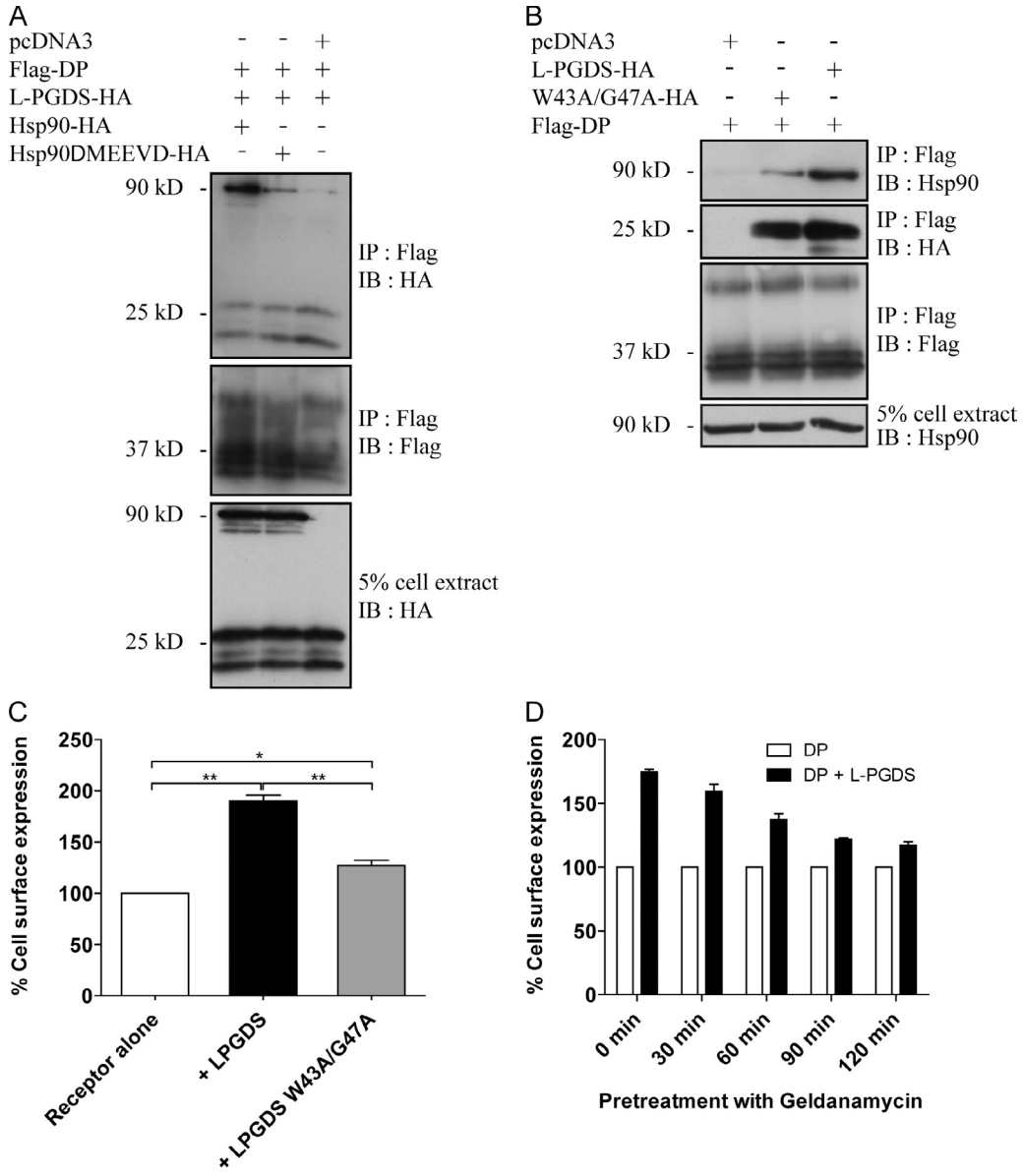

Figure 7. **L-PGDS promotes the interaction between DP1 and Hsp90.** (A) HEK293 cells were transiently transfected with the indicated combinations of pcDNA3, Flag-DP1, L-PGDS-HA, Hsp90-HA, or Hsp90ΔMEEVD-HA mutant constructs. Immunoprecipitation (IP) of the receptor was performed using a Flag-specific monoclonal antibody, and immunoblotting (IB) was performed with Flag-specific polyclonal or peroxidase-conjugated anti-HA antibodies. (B) HEK293 cells were transiently transfected with Flag-DP1 together with pcDNA3, L-PGDS–HA, or L-PGDS–W43A/G47A-HA. Immunoprecipitation of the receptor was performed using a Flag-specific monoclonal antibody, and immunoblotting was performed using peroxidase-conjugated anti-HA or polyclonal anti-Flag antibodies. Endogenous Hsp90 was detected using an Hsp90-specific polyclonal antibody. Blots shown are representative of three separate experiments. Blots shown were spliced but came from the same gels. (C) Cell surface expression of DP1 was measured by ELISA in HEK293 cells transiently transfected for 48 h with Flag-DP1 together with pcDNA3, pcDNA3–L-PGDS–HA, or pcDNA3–L-PGD–W43A/G47A-HA. Results are shown as the percentage of cell surface expression of DP1 when cells were transfected with L-PGDS or L-PGDS–W43A/G47A compared with cell surface expression of DP1 when transfected with pcDNA3. (D) HEK293 cells were transiently transfected for 48 h with Flag-DP1 together with pcDNA3 or pcDNA3–L-PGDS–HA, treated with 10 µM geldanamycin over a time course of 2 h, and cell surface expression of DP1 was measured by ELISA. All values are the means ± SE from at least three separate experiments. *, $P < 0.05$; **, $P < 0.01$.

transfected L-PGDS and (b) a decreased interaction between the molecular chaperone and L-PGDS results in a diminished Hsp90–DP1 receptor interaction as demonstrated by data obtained with the L-PGDS–W43A/G47A mutant.

The functional consequence of decreased L-PGDS–Hsp90 interaction on DP1 export was then assessed. Wild-type L-PGDS promoted DP1 cell surface expression by ∼80% in these experiments compared with when the receptor is expressed alone (Fig. 7 C). In contrast, the L-PGDS–W43A/G47A mutant increased DP1 export by only ∼30%. Altogether, these results indicate that L-PGDS, through a site comprising Trp43 and Gly47, interacts with the MEEVD residues of Hsp90 to promote a DP1–L-PGDS–Hsp90 complex that favors the export of the receptor to the cell surface.

To further confirm the importance of Hsp90 in this effect, we measured DP1 levels at the cell surface in HEK293 cells transfected with Flag-DP1 together with pcDNA3 or pcDNA3–L-PGDS–HA after a time course pretreatment of the cells with

geldanamycin, an Hsp90 inhibitor. Fig. 7 D shows that the longer the treatment with geldanamycin, the more the L-PGDS–mediated increase in cell surface expression of DP1 was prevented, indicating that Hsp90 is indeed involved in the promotion of DP1 export by L-PGDS.

The L-PGDS–W43A/G47A mutant protein appeared as stable as the wild-type protein in Western blot analysis (Figs. 6 E and 7 B). Additional experiments were performed to verify whether it was not mistargeted intracellularly or misfolded. Confocal microscopy showed that both the mutant and wild-type L-PGDS proteins displayed indistinguishable intracellular distribution in HEK293 cells with a predominant association with vesicular structures in the cytoplasm and an increased concentration within the perinuclear region (Fig. 8 A). Production of PGD_2 in vitro and in HEK293 cells by the L-PGDS–W43A/G47A mutant was not significantly different from that of wild-type L-PGDS (Fig. 8, B and C). These data show that the W43A/G47A mutations did not affect the intracellular localization and enzymatic activity of L-PGDS.

LPGDS increases DP1-mediated ERK1/2 signaling

The functional consequence of the DP1–L-PGDS interaction was next assessed on DP1 signaling. We recently showed that DP1 stimulation results in ERK1/2 activation (Labrecque et al., 2013). Time course analyses of ERK1/2 activation after stimulation of endogenous DP1 or β_2-adrenergic receptors were performed in HeLa cells that were transfected with control or L-PGDS siRNAs (Fig. 9 A). Depletion of L-PGDS caused a significant reduction in DP1-mediated ERK1/2 activation ranging from 35 to 70% for time points between 0 and 15 min of agonist stimulation (Fig. 9 A, left) but had no effect on the β_2-adrenergic receptor ERK1/2 signaling (Fig. 9 A, right). We also verified the effect of coexpressing wild-type L-PGDS or L-PGDS–C65A on DP1-mediated ERK1/2 activation. HEK293 cells transfected with the indicated combinations of pcDNA3, L-PGDS, L-PGDS–C65A, and DP1 constructs were stimulated or not stimulated with PGD_2 (Fig. 9 B, left). Transfection of L-PGDS or L-PGDS–C65A promoted PGD_2-induced ERK1/2 activation by ∼75% and ∼70%, respectively, in the absence of DP1 transfection (Fig. 9 B, compare eighth and ninth lanes with seventh lane). Both forms of L-PGDS induced a twofold increase in ERK1/2 activation by the transfected DP1 (Fig. 9 B, eleventh and twelfth lanes compared with tenth lane). In contrast, isoproterenol-induced ERK1/2 activation by the β_2-adrenergic receptor was not modulated by coexpression of L-PGDS (Fig. 9 B, right). These data with overexpressed L-PGDS support our results obtained with the L-PGDS siRNAs on endogenous DP1 and β_2-adrenergic receptor signaling. The ability of L-PGDS–C65A to promote DP1-mediated ERK1/2 signaling to the same extent as the wild-type counterpart indicates that the PGD_2 synthase activity of L-PGDS is not involved in regulating the DP1-induced ERK1/2 signaling when exogenous PGD_2 is added.

Interestingly, confocal microscopy in HeLa cells showed that phospho-ERK1/2 was colocalized with L-PGDS in the perinuclear region when the synthase was transfected (Fig. 10 A). Treatment of cells with an inhibitor of L-PGDS (AT-56) or with a DP1 antagonist (BWA868C) both prevented L-PGDS–induced ERK1/2 activation (Fig. 10, A and B). This indicates that expression of L-PGDS in HeLa cells results in PGD_2 formation that stimulates endogenous DP1 leading to ERK1/2 activation in the perinuclear region.

The strong colocalization observed between ERK1/2 and L-PGDS prompted us to verify whether L-PGDS and ERK1/2 could be found in a complex. Noteworthily, Fig. 10 C shows that endogenous L-PGDS coimmunoprecipitated endogenous activated ERK1/2, in addition to endogenous DP1 (Fig. 3 C). Moreover, L-PGDS strongly promoted the coimmunoprecipitation between DP1 and endogenous ERK1/2 in HEK293 cells in basal conditions (Fig. 10 D, forth lane vs. third lane) and after agonist stimulation (Fig. 10 D, seventh lane vs. sixth lane). Altogether, our data suggest that DP1, ERK1/2, and L-PGDS are part of a DP1 signaling complex in the perinuclear region.

Discussion

The mechanisms involved in the folding, maturation, and export of newly synthesized GPCRs to the cell surface still remain poorly understood. Misfolded proteins are retained in the ER where they can be targeted for degradation or assisted by molecular chaperones in proper folding. Our previous study conducted on DP1 revealed such retention of misfolded or unassembled forms of the receptor (Parent et al., 2010). In the present study, we have demonstrated that L-PGDS interacts with DP1 to regulate the export of the receptor through Hsp90 and to favor a DP1–ERK1/2 signaling complex, thus uncovering new roles for L-PGDS.

Our confocal microscopy data indicated that DP1 and L-PGDS are present in perinuclear compartments, such as the ER and TGN, corroborating our previous studies (Parent et al., 2010; Mathurin et al., 2011; Labrecque et al., 2013). Given the fact that the two proteins are located in the same subcellular compartments and that L-PGDS produces PGD_2 that binds to DP1, we investigated a possible interaction between the two proteins. Our experiments showed a direct interaction between L-PGDS and DP1, which was confirmed by coimmunoprecipitations between overexpressed proteins in HEK293 cells and endogenous proteins in HT-29 cells. Interestingly, total expression of the receptor protein and the maturation (glycosylation) pattern of DP1 were not affected by L-PGDS, suggesting that the latter does not regulate the biogenesis/stability and export of DP1 at the ER. This is in contrast to what we reported for the role of ANKRD13C in DP1 expression (Parent et al., 2010). Our data suggest that L-PGDS acts on DP1 after Golgi modifications. Other GPCRs, such as the μ-δ opioid receptor heterodimer, which are class A GPCRs, like DP1, have been shown to be trapped in the Golgi (Petäjä-Repo et al., 2002; Leskelä et al., 2007; Décaillot et al., 2008). RTP4 (receptor transport protein 4) was reported to participate in the proper folding of the μ-δ heterodimer, allowing it to be routed out of the Golgi apparatus to the cell surface (Décaillot et al., 2008).

L-PGDS promotes the export of DP1 specifically, having no effect on CRTH2. This could be relevant to the fact that even

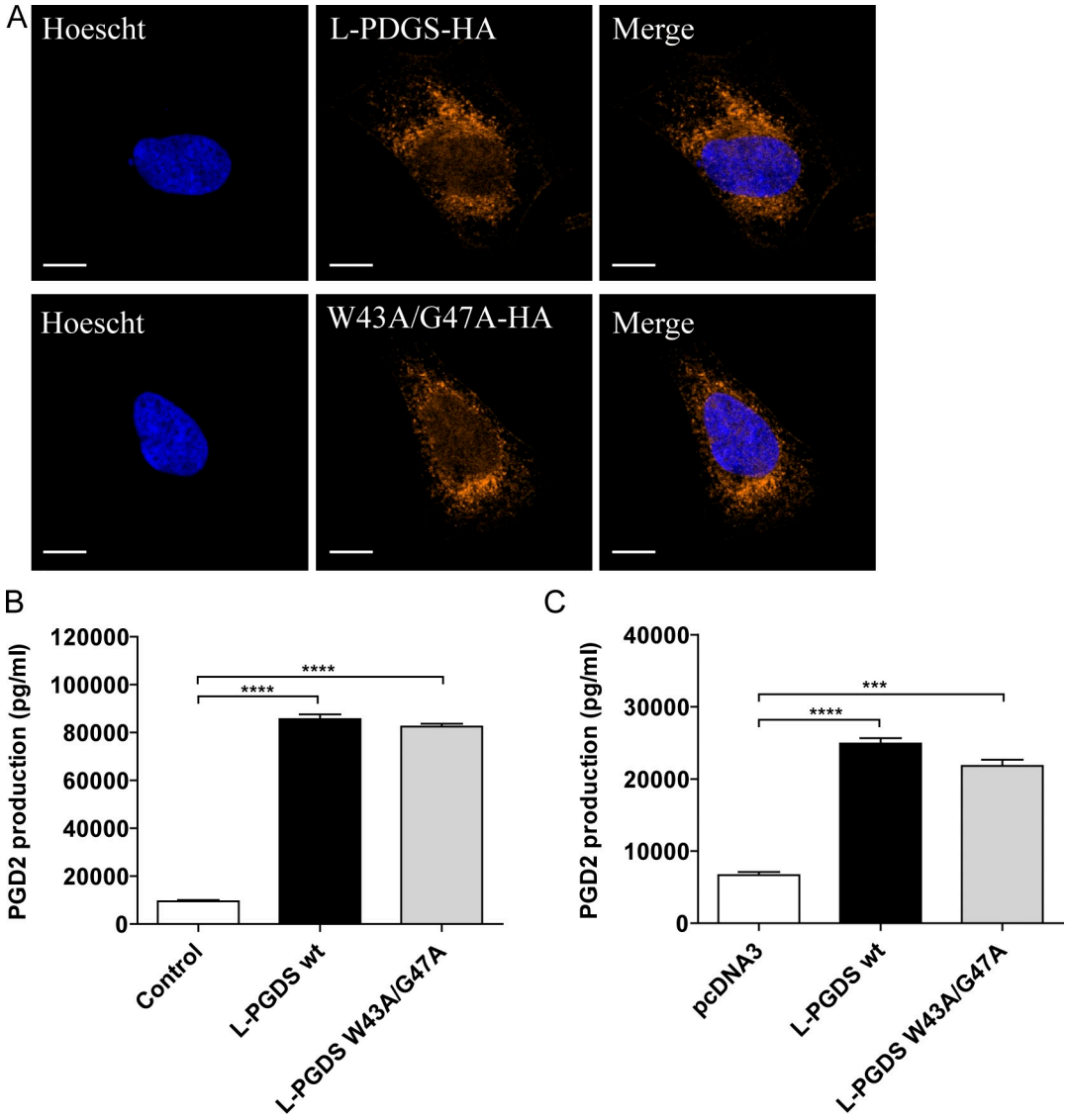

Figure 8. **Intracellular distribution and PGD_2 synthase activity of the L-PGDS–W43A/G47A mutant.** (A) HEK293 cells were transiently transfected with pcDNA3–L-PGDS–HA or pcDNA3–L-PGDS–W43A/G47A-HA for 48 h. The cells were then fixed and prepared for confocal microscopy as described under Materials and methods. The L-PGDS constructs were visualized using HA-specific monoclonal and Alexa Fluor 546–conjugated anti–mouse IgG antibodies (orange). An overlay of staining patterns of the orange-labeled L-PGDS or its mutant and the nuclei are shown (merge). Bars, 10 µM. (B) PGD_2 production by purified GST, GST–L-PGDS, and GST–L-PGDS–W43A/G47A was measured in vitro in the presence of 0.5 µM PGH_2 for 1 min. The reactions were stopped with 0.4 mg/ml $SnCl_2$, and PGD_2 was measured with commercial enzyme-linked immunoassays as described under Materials and methods. (C) HEK293 cells were transiently transfected with pcDNA3, L-PGDS, or L-PGDS–W43A/G47A for 48 h. Cells were then incubated with 5 µM PGH_2 for 15 min. Supernatants were assessed for PGD_2 production by commercial enzyme-linked immunoassays as described under Materials and methods. All values are the means ± SE from at least three separate experiments. wt, wild type. ***, $P < 0.001$; ****, $P < 0.0001$.

though the two receptors bind the same PG, they differ completely in their amino acid sequence and their cellular role (Narumiya et al., 1999; Oguma et al., 2008; Schuligoi et al., 2010; Chiba et al., 2011). CRTH2 is a receptor that is efficiently targeted at the cell membrane (Parent et al., 2010) and may not need further assistance in its export. One could speculate that DP1 could signal from the cell surface and from intracellular compartments as shown for other GPCRs for lipid mediators (Zhu et al., 2006), whereas CRTH2 could be primarily involved in signaling from the cell membrane. Specificity of the L-PGDS function is further supported by the lack of effect of H-PGDS on targeting DP1 to the cell surface. This can be expected, considering that L-PGDS and H-PGDS are structurally different (Zhou et al., 2010) and are mainly expressed in different cell types. Specificity of L-PGDS is also demonstrated by its inability to modulate the export of the other GPCRs tested in the present study.

The L-PGDS–mediated increase in DP1 export is independent of the PGD_2 synthase activity of the enzyme. This is indicated by the ability of the L-PGDS–C65A mutant to increase the cell surface expression of DP1 as efficiently as wild-type L-PGDS. This prompted us to look for mechanisms that could explain this new L-PGDS function. Although L-PGDS is structurally unrelated to TPR domains, the presence of a motif in its sequence that was reminiscent of the consensus TPR sequence found in H sp90 co-chaperones suggested that Hsp90 might be an interacting partner of L-PGDS. Interestingly, our data revealed

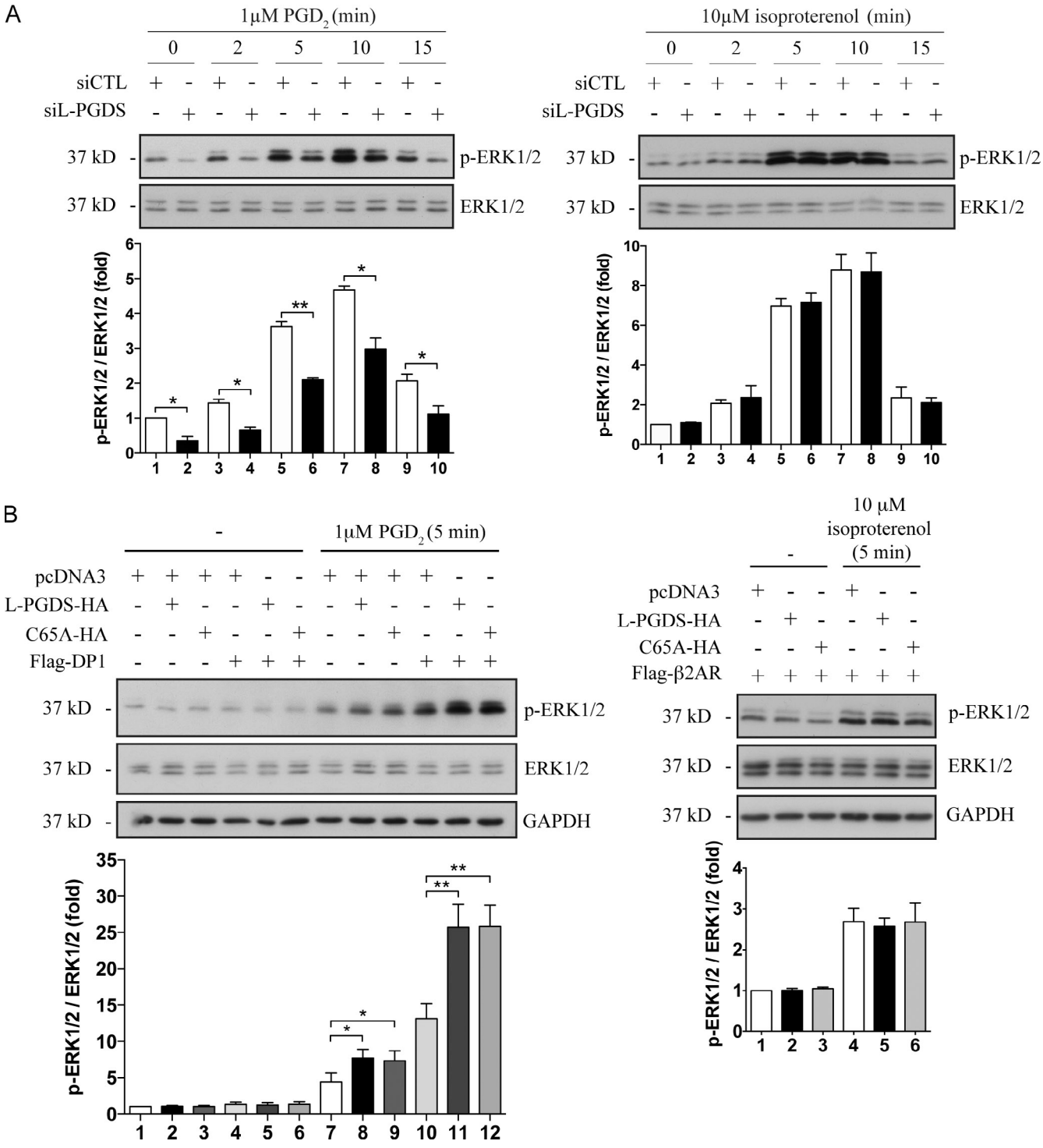

Figure 9. **L-PGDS promotes ERK1/2 activation.** (A) HeLa cells were transfected with the indicated siRNA for 48 h, serum starved overnight, and stimulated or not stimulated with 1 μM PGD_2 (left) or 10 μM isoproterenol (right) for the indicated times. siCTL, control siRNA. (B) HEK293 cells were transfected with pcDNA3, L-PGDS, L-PGDS–C65A, DP1 (left), or β2AR (right) for 24 h, serum starved overnight, and stimulated or not stimulated with 1 μM PGD_2 (left) or 10 μM isoproterenol (right) for 5 min. All assays were performed as described in Materials and methods. Protein levels were assessed by Western blotting using p-ERK1/2 and ERK1/2 antibodies. Bar graphs show densitometry analyses performed on four different experiments. Phospho-ERK1/2 pixels were normalized to total ERK1/2 pixels, and results are presented as the fold of these values (means ± SE) over that of the first lane, which was arbitrarily set as 1. *, $P < 0.01$; **, $P < 0.005$.

that L-PGDS, through a domain including Trp43 and Gly47, binds to the C-terminal MEEVD motif of Hsp90. The L-PGDS interaction with the MEEVD domain of Hsp90 may constitute a new mechanism of Hsp90 binding. Co-chaperones that bind the MEEVD motif of Hsp90 are recognized to have little effect on its intrinsic ATPase activity, as opposed to the N-terminal binding co-chaperones that can inhibit or activate its ATPase activity (Jackson, 2013). It is thus unlikely that L-PGDS promotes the

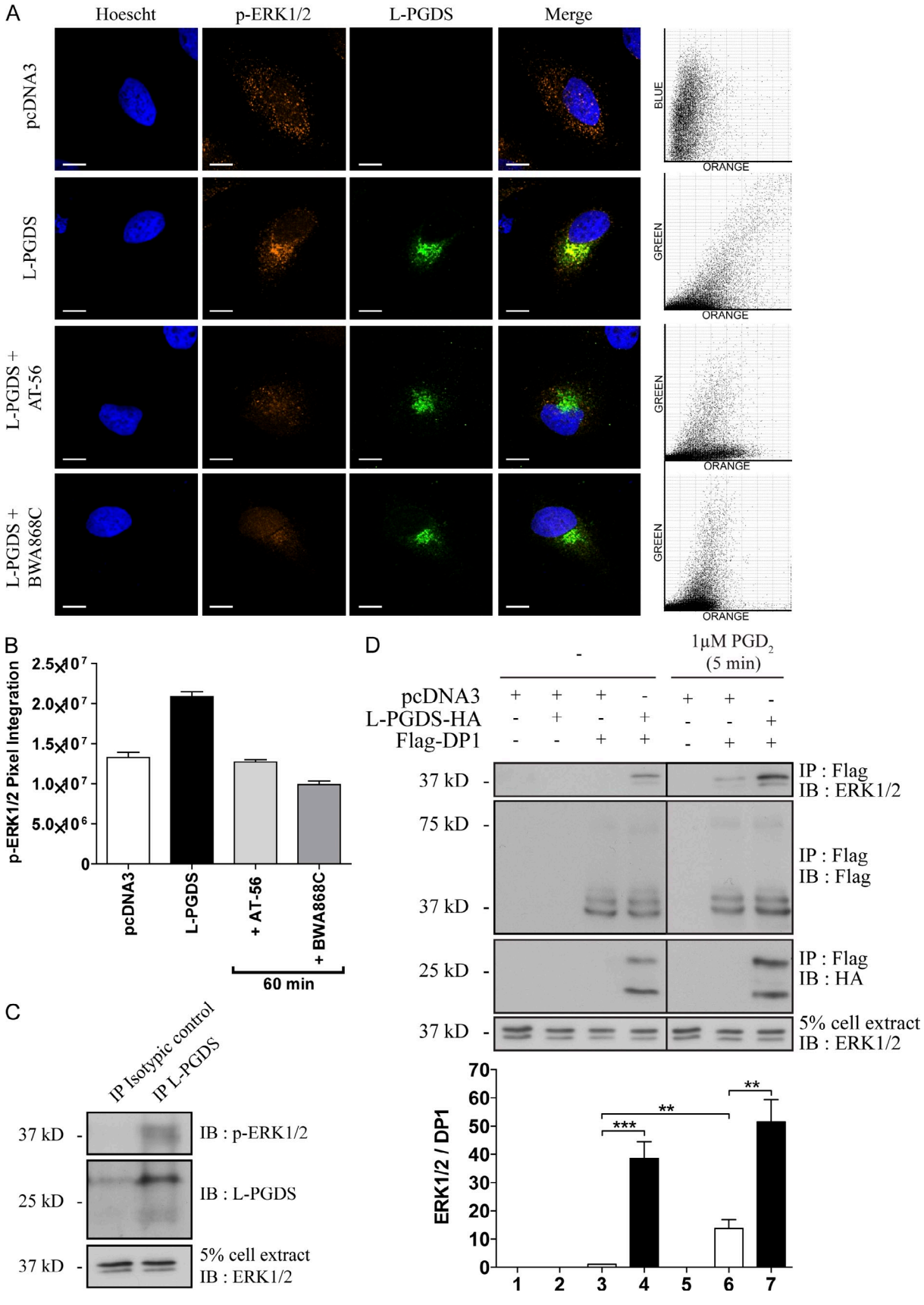

Figure 10. **L-PDS is part of a DP1–ERK1/2 signaling complex in the perinuclear region.** (A) HeLa cells were transiently transfected with pcDNA3 or pcDNA3–L-PGDS–HA for 24 h, serum starved overnight, and treated with 100 µM AT-56 or 1 µM BWA868C for 60 min. The cells were then prepared for confocal microscopy as described under Materials and methods. L-PGDS was visualized using HA-specific monoclonal and Alexa Fluor 488–conjugated

ATPase activity of Hsp90. It is more probable that L-PGDS has a co-chaperone–like role to promote Hsp90 association with specific complexes. L-PGDS may act as a DP1-specific co-chaperone.

We thus explored the possible assembly of an Hsp90–L-PGDS–DP1 complex. The Hsp90–DP1 interaction was observed only when L-PGDS was cotransfected in HEK293 cells, which do not express detectable endogenous L-PGDS levels. In the presence of L-PGDS, the interaction between Hsp90ΔMEEVD and DP1 was diminished compared with wild-type Hsp90. Moreover, the interaction between Hsp90 and DP1 was greater with coexpression of wild-type L-PGDS than with the L-PGDS–W43A/G47A mutant. Altogether, these data indicate that the L-PGDS–Hsp90 interaction is required for the association between Hsp90 and DP1 and export of the receptor. Involvement of Hsp90 in L-PGDS–mediated promotion of DP1 export is further supported by the ability of geldanamycin, an Hsp90 inhibitor, to inhibit the L-PGDS effect.

It has been shown that Hsp90 is implicated in facilitating G protein–coupled pathways (Garcia-Cardeña et al., 1998); however, only a few GPCRs have been reported to interact with and be regulated by Hsp90 thus far. In each case, Hsp90 regulates the receptors in different ways. Hsp90 is involved in maintaining the PAR1 receptor's C tail in proper conformation for signal transduction (Pai et al., 2001). It is also known to modulate trafficking of the α_{2C}-adrenergic receptor via a low-temperature inhibition of its activity (Filipeanu et al., 2011). Hsp90 was shown to regulate the stability of GPCR kinases (Luo and Benovic, 2003). It was also reported to interact in a complex with XPORT, an ER resident protein, which functions as a molecular chaperone with Hsp90 during biosynthesis and transport of rhodopsin (Rosenbaum et al., 2011). Furthermore, Hsp90 was demonstrated to function as a scaffold for the cannabinoid CB2 receptor to keep the receptor in proximity with its signaling components that are required for receptor-mediated cell migration via the $G_{\alpha i}$–Rac1 pathway (He et al., 2007). By analogy, it will be interesting to determine whether Hsp90 plays such a role in the formation of a DP1–L-PGDS–ERK1/2 signaling complex or in the interaction with other effectors and regulators of DP1 in our system. In addition to recruiting Hsp90 to DP1 complexes, L-PGDS may have chaperone activity for the receptor itself. This is consistent with its role in the central nervous system in which L-PGDS, also known as β-trace, functions to keep Aβ from misfolding and aggregating under normal conditions in the healthy brain, thus preventing early onset and progression of Alzheimer's disease (Kanekiyo et al., 2007).

Surprisingly, DP1 coexpression increased PGD_2 production by L-PGDS. The intracellular L-PGDS–DP1 interaction raises the intriguing possibility of an intracrine signaling mechanism (Zhu et al., 2006; Vaniotis et al., 2011; Tadevosyan et al., 2012) in which the mutual L-PGDS and DP1 regulation could trigger signaling pathways from intracellular DP1 in response to its agonist synthesized by the interacting L-PGDS. We thus report a new mechanism in which a GPCR interacts with, and activates, the enzyme that produces its agonist at the intracellular level.

Our data put forward interesting potential functional consequences for the DP1–L-PGDS cooperativity. DP1 promotes L-PGDS activity, which results in PGD_2 production and DP1 signaling. In turn, L-PGDS, through Hsp90, would bestow proper conformation or assembly of DP1 for its export. Our results also suggest that L-PGDS could favor assembly of DP1 with effectors, as indicated by its ability to promote the formation of L-PGDS–ERK1/2 complexes. Because (a) L-PGDS interacts and localizes in the perinuclear region with DP1 but not at the plasma membrane, (b) ERK1/2 activation is maximal and transient after 5 min of DP1 stimulation (Labrecque et al., 2013), much faster than the slow internalization of the receptor, which peaks after 60 min of receptor activation (Gallant et al., 2007), (c) DP1 increases PGD_2 production by L-PGDS, and (d) that L-PGDS–induced ERK1/2 activation detected in the perinuclear region depends on DP1 activation and on synthesis of PGD_2, which has a short half-life, we postulate that L-PGDS might be found in a complex with DP1 and ERK1/2 as part of a DP1–L-PGDS intracrine signaling complex in the perinuclear region. COX-1 is located in the ER and perinuclear membranes, whereas COX-2 resides predominantly in the perinuclear envelope (Morita et al., 1995). Thus, an intracrine DP1–L-PGDS mechanism in the perinuclear region could ensure efficient response during inflammatory or cancerous conditions, for example, that induce cyclooxygenase activity to generate PGH_2, the L-PGDS substrate, in the vicinity of the DP1–L-PGDS complex.

The DP1–L-PGDS interaction could thus possibly promote DP1 signaling in two ways: by assembling an intracrine signaling complex as just described and by promoting DP1 export to assure proper DP1 cell surface expression for plasma membrane signaling in response to autocrine or paracrine production of PGD_2. Indication of autocrine or paracrine activation of DP1 in our system was provided by the increase in detection of L-PGDS–mediated DP1 export in presence of BWA868C and dynamin-K44A, which inhibit PGD_2-induced internalization of cell surface receptors. Unfortunately, existing DP1 antagonists are not characterized in terms of cell permeability or intracellular uptake to distinguish pharmacologically between the signaling from DP1 at the plasma membrane versus intracellular DP1. Our results should generate interest in

anti–mouse IgG antibodies (green). Endogenous p-ERK1/2 was detected using a p-ERK1/2–specific polyclonal antibody and Alexa Fluor 546–conjugated anti–rabbit IgG (orange). An overlay of staining patterns of the orange-labeled p-ERK1/2 and green-labeled L-PGDS and the corresponding fluorograms are shown. Bars, 10 µM. (B) Mean pixel integration of p-ERK1/2 of ≥10 different cells was determined using the FluoView 2.0 software (Olympus). (C) The same L-PGDS immunoprecipitation (IP) reaction as in Fig. 3 C performed using L-PGDS–specific monoclonal or isotypic control IgG antibodies was used, and immunoblotting (IB) was performed using p-ERK1/2– or ERK1/2-specific polyclonal or L-PGDS–specific polyclonal antibodies. (D) HEK293 cells were transiently transfected with pcDNA3, L-PGDS–HA, or Flag-DP1 constructs. Immunoprecipitation of DP1 was performed using a Flag-specific monoclonal antibody, and immunoblotting was performed using peroxidase-conjugated anti-HA– or p-ERK1/2–specific polyclonal antibodies. Black lines indicate that intervening lanes have been spliced out. Bar graph shows densitometry analyses performed on four different experiments. ERK1/2 pixels were normalized on the receptor pixels, and results are presented as the fold of these values over that of the third lane (means ± SE), which was arbitrarily set as 1. **, $P < 0.005$; ***, $P < 0.0005$.

developing/characterizing such molecules and to study particular cell responses generated by the two different DP1 populations. DP1 and L-PGDS did not modulate their mutual levels of protein expression in the present report. However, data were obtained in context of transfected proteins under the control of the cytomegalovirus promoter. Future studies will address whether the DP1–L-PGDS signaling that results in ERK1/2 activation leads to the regulation of expression of particular genes, including that of DP1 and L-PGDS themselves.

In summary, we have demonstrated the cooperativity between a GPCR and the synthase of its agonist: the receptor promotes the activity of the enzyme, which in turn increases the export of the receptor through an Hsp90-dependent mechanism and favors assembly of DP1–ERK1/2 complexes. We have provided evidence suggesting that the intracellular DP1–L-PGDS interaction might be involved in a novel intracrine signaling mechanism.

Materials and methods

Reagents

The Flag-specific monoclonal (M1 and M2) as well as polyclonal anti-Flag antibodies, rabbit anti-actin antibody (A2066), alkaline phosphatase–conjugated goat anti–mouse antibodies, and the alkaline phosphatase substrate kit were purchased from Sigma-Aldrich. The monoclonal anti-HA (16B12) was obtained from Covance. The monoclonal anti-HA–peroxidase high affinity antibody (3F10) was obtained from Roche. The anti-Myc–peroxidase high affinity polyclonal antibody was purchased from Abcam. The anti-GST polyclonal antibody was purchased from Bethyl Laboratories, Inc. The monoclonal anti-His, anti-Grp94 (2104), phospho-p44/p42 MAPK (Erk1/2; Thr202/Tyr204), and total p44/42 MAPK (Erk1/2) antibodies were obtained from Cell Signaling Technology. The anti-TGN46 was obtained from Novus Biologicals (NB110-40769). The polyclonal anti-Myc, normal mouse IgG isotypic control antibody, and anti-GAPDH and anti-Hsp90 antibodies as well as the protein G–agarose beads were purchased from Santa Cruz Biotechnology, Inc. The polyclonal and monoclonal anti–L-PGDS antibodies, PGD_2, AT-56, BWA868C, and PGH_2 were obtained from Cayman Chemical Co. MK-0524 was obtained from Axon Medchem BV. Alexa Fluor 633 goat anti–mouse, Alexa Fluor 647 goat anti–rat, Alexa Fluor 546 goat anti–rabbit, Alexa Fluor 488 goat anti–rabbit, and ProLong Gold antifade reagent were purchased from Invitrogen. Geldanamycin was purchased from Enzo Life Sciences (El-280).

Plasmid constructs

The cDNA fragment coding for the C terminus of human DP1 (amino acids 331–359) was generated by PCR using the high fidelity DNA polymerase (Phusion; New England Biolabs, Inc.) from the pcDNA3-HA-DP1 construct (Gallant et al., 2005). The PCR fragment was digested with EcoRI and XhoI and ligated into the pGEX4T1 vector (GE Healthcare). The ICL1 (amino acids 46–57) and ICL2 (amino acids 129–150) fragments of DP1 were generated by annealing two pairs of complementary oligonucleotides. Equal quantities of oligonucleotides were mixed and denatured by boiling for 5 min. The mix was then incubated at room temperature for 30 min to allow hybridization, digested with EcoRI and XhoI, and ligated into the pGEX4T1 vector digested with the same enzymes. The ICL3 (amino acids 217–262) fragment of DP1 was amplified by PCR, digested with EcoRI and XhoI, and ligated into the pGEX4T1 vector digested with the same enzymes. All site-directed mutagenesis was performed by PCR using the Phusion high fidelity DNA polymerase. The L-PGDS–C65A-HA mutant was prepared from the pcDNA3–L-PGDS–HA construct (Mathurin et al., 2011) by using the following primers: L-PGDS forward, 5′-ATCGGATCCATGGCTACTCATCACACG-3′; L-PGDS–C65A reverse, 5′-CCACCACAGACTTGGCCATGGACAACGCC-3′; L-PGDS–C65A forward, 5′-GGCGTTGTCCATGGCCAGGTCTGTGGTGG-3′; and L-PGDS reverse, 5′-GATGAATTCCTAAGCGTAGTCTGGGACGTCGTATGGGTATTGTTCCGTCATGCACTTATC-3′. The fragments were ligated by PCR extension method. The full-length fragment was digested with BamHI and EcoRI and ligated into the pcDNA3 vector digested with the same enzymes. The L-PGDS–W43A/G47A-HA mutant was prepared from the pcDNA3–L-PGDS–HA construct by using the following primers: L-PGDS–W43A/G47A forward, 5′-CTGGGGCGCGCATTCAGCGCGGCACTCGCCTCC-3′; L-PGDS–W43A/G47A reverse, 5′-GGAGGCGAGTGCCGCGCTGAATGCGCGCCCCAG-3′; and L-PGDS forward and L-PGDS reverse as described previously in this paragraph. The fragments were ligated by PCR extension method. The full-length and W43A/G47A mutant fragment were digested with BamHI and EcoRI and ligated in the pcDNA3 and pGEX4T1 vectors digested with the same enzymes. The pcDNA3-dynamin-K44A construct was a gift of J.L. Benovic (Thomas Jefferson University, Philadelphia, PA). The full-length Hsp90 and ΔMEEVD mutant cloned into pcDNA3.1-N-HA were provided by Y. Matsuura (Research Institute for Microbial Diseases, Osaka University, Osaka, Japan). A PCR fragment corresponding to the cDNA coding for full-length L-PGDS was inserted into the pRSETA expression vector (Invitrogen) as described previously (Mathurin et al., 2011). The wild-type arginine vasopressin receptor 2 and its intracellularly trapped W164S and Y205C mutant constructs were provided by M. Bouvier (University of Montreal, Montreal, Quebec, Canada).

Cell culture and transfections

HEK293 (human embryonic kidney 293), human colorectal adenocarcinoma (HT-29), and HeLa cells were maintained in DMEM (Invitrogen) supplemented with 10% fetal bovine serum at 37°C in a humidified atmosphere containing 5% CO_2. Transient transfection of HEK293 and HeLa cells grown to 50–70% confluence was performed using the TransIT-LT1 reagent (Mirus Bio LLC) according to the manufacturer's instructions. The total DNA amount was kept constant by adding an empty pcDNA3 vector per plate.

Immunoprecipitation

HEK293 cells were transiently transfected with the indicated constructs and were maintained as described in the previous paragraph for 48 h. Where indicated, cells were incubated in the presence of 1 µM PGD_2 for the desired times before harvesting. The cells were then washed with ice-cold PBS and harvested in 200 µl lysis buffer (150 mM NaCl, 50 mM Tris, pH 8.0, 0.5% deoxycholate, 0.1% SDS, 10 mM $Na_4P_2O_7$, 1% IGEPAL, and 5 mM EDTA or 1 mM $CaCl_2$ depending on the antibody used for the assay) supplemented with protease inhibitors (9 nM pepstatin, 9 nM antipain, 10 nM leupeptin, and 10 nM chymostatin; Sigma-Aldrich). After 45 min of incubation in lysis buffer at 4°C, the lysates were centrifuged for 15 min at 14,000 *g* at 4°C. Proteins were immunoprecipitated for 60 min using 1 µg of specific antibodies before adding 40 µl of 50% protein G–agarose beads to the lysates for 30 min. Samples were then centrifuged for 2 min in a microcentrifuge and washed three times with 1 ml lysis buffer. Immunoprecipitated proteins were eluted by addition of 35 µl SDS sample buffer followed by an incubation of 60 min at room temperature. Initial lysates and immunoprecipitated proteins were analyzed by SDS-PAGE and immunoblotting with specific antibodies. Endogenous immunoprecipitations were performed in HeLa and HT-29 cells. Cells were harvested and processed as described for HEK293 cells except proteins were immunoprecipitated overnight using 5 µg L-PGDS–specific or appropriate control antibodies and 40 µl of 50% protein G–agarose beads.

Recombinant protein production and pull-down analysis

To produce GST-tagged proteins, PCR fragments corresponding to the C terminus and intracellular loops of DP1 as well as L-PGDS and its mutant W43A/G47A were inserted in the pGEX-4T1 vector (GE Healthcare), and the fusion proteins were produced in C41 (DE3) *Escherichia coli* strain (OverExpress; Avidis) by following the manufacturer's instructions. Gluthatione–Sepharose 4B (GE Healthcare) was used for protein purification, and the purified recombinant proteins were analyzed by SDS-PAGE followed by Coomassie brilliant blue R-250 staining. The His-tagged L-PGDS construct was produced and purified using nickel–nitrilotriacetic acid-agarose resin (QIAGEN) as indicated by the manufacturer, as described previously (Mathurin et al., 2011). 5 µg of each gluthatione-Sepharose–bound GST-tagged fusion protein was incubated with 5 µg of the purified His-tagged full-length proteins in binding buffer (10 mM Tris-HCl, pH 7.4, 150 mM NaCl, 1 mM EDTA, 10% glycerol, 0.5% IGEPAL, and 2 mM DTT) supplemented with protease inhibitors (9 nM pepstatin, 9 nM antipain, 10 nM leupeptin, and 10 nM chymostatin). The binding reactions were then washed three times with binding buffer. SDS sample buffer was added to the each reaction before boiling the tubes for 5 min. All reactions were analyzed by Western blotting using specific antibodies as indicated. To perform Histone pull-down assays, purified His-Hsp90-α (catalog #10202) and purified L-PGDS (catalog #10006788) were purchased from Cayman Chemical Co. His-Hsp90 was preincubated with nickel–nitrilotriacetic acid-agarose resin for 30 min before adding the purified L-PGDS for 1 h. The binding reactions were then washed three times with binding buffer. SDS sample buffer was added to the each reaction. All reactions were analyzed by Western blotting using specific antibodies as indicated.

Immunofluorescence staining and confocal microscopy
For colocalization experiments, HEK293 cells were plated in 6-well plates at a density of 1.5×10^5 cells/well. Cells were then transiently transfected with the indicated constructs, transferred onto coverslips coated with 0.1 mg/ml poly-L-lysine (Sigma-Aldrich) the following day, and further grown overnight. Cells were fixed with 4% paraformaldehyde in PBS, washed with PBS, permeabilized with 0.1% Triton X-100 in PBS, and blocked with 0.1% Triton X-100 in PBS containing 5% nonfat dry milk. Cells were then incubated with primary antibodies diluted in blocking solution for 60 min, washed twice with PBS, blocked again with 0.1% Triton X-100 in PBS containing 5% nonfat dry milk, and incubated with the appropriate secondary antibodies diluted in blocking solution. The cells were washed three times with PBS, and the coverslips were mounted using ProLong Gold antifade reagent. Confocal microscopy was performed at room temperature using a scanning confocal microscope (FV1000; Olympus) coupled to an inverted microscope with a Plan Apochromat 63× oil immersion objective lens, NA 1.42 (Olympus). Following acquisition, images were pseudocolored using the FV10-ASW 2.0.1.0 viewer software (Olympus). HeLa cells were plated in 6-well plates at a density of 1.5×10^6 cells/well directly onto coverslips and transiently transfected with the indicated constructs the same day. After 24 h, cells were starved overnight in DMEM medium containing 0.5% BSA and 20 mM Hepes. Cells were then left untreated or treated with 1 µM BWA868C or 100 µM AT-56 for the indicated time periods at 37°C in starving medium and further processed as described for HEK293 cells.

Measurement of cell surface receptor expression
For quantification of cell surface receptor expression, 6×10^5 HEK293 cells were plated in 24-well plates pretreated with 0.1 mg/ml poly-L-lysine. Cells were transfected with the indicated constructs and maintained for an additional 48 h. Cells were then fixed in 3.7% formaldehyde/TBS (20 mM Tris, pH 7.5, and 150 mM NaCl) and washed twice with TBS. Nonspecific binding was blocked with TBS containing 1% BSA for 45 min. A monoclonal $Flag_{M1}$-specific antibody was then added at a dilution of 1:2,000 in 1% TBS-BSA for 60 min. Following the incubation, cells were washed three times and blocked again with 1% TBS-BSA for 15 min. Cells were then incubated with an alkaline phosphatase–conjugated goat anti–mouse antibody at a 1:10,000 dilution in 1% TBS-BSA for 60 min. The cells were then washed three times, and 250 µl of a colorimetric alkaline phosphatase substrate was added. The plates were incubated at 37°C for 30 min followed by the addition of 250 µl NaOH (0.4 M) to stop the reaction. A 100-µl aliquot of the colorimetric reaction was collected, and the absorbance was measured at 405 nm using a spectrophotometer (Titertek Multiskan MCC/340; Labsystems).

ERK1/2 phosphorylation
HeLa cells or HEK293 cells were seeded in 60-mm dishes at 4.5×10^5 and 7×10^5 cells per dish, respectively, and grown for 24 h before transfection with the indicated constructs. 24 h after transfection, cells were starved overnight in DMEM supplied with 0.5% BSA and 20 mM Hepes, pH 7.5, and then treated with 1 µM PGD_2 for the indicated times. The reactions were stopped with 900 µl of sample buffer (62.5 mM Tris, pH 7.0, 2% wt/vol SDS, 10% glycerol, 50 mM DTT, and 0.01% wt/vol bromophenol blue) and sonicated. After sonication, samples were analyzed by Western blotting using phospho-p42/44 and secondary horseradish peroxidase–conjugated anti–rabbit antibodies. Experiments were performed at least three times for each condition. For experiments using siRNAs, HeLa cells were seeded and transfected with the indicated siRNA on the same day.

siRNA assays
The synthetic oligonucleotide targeting the human L-PGDS (*PTGDS*) gene (siRNA ID s11446) was purchased from Ambion. The negative control siRNA was also purchased from Ambion (Silencer Negative Control 1; catalog number 4390843). HeLa cells stably expressing the HA-DP1 receptor were transfected with 200 nM oligonucleotide using the Lipofectamine 2000 transfection reagent (Invitrogen) according to the manufacturer's instructions. Protein expression was assessed by Western blotting at 72 h after transfection.

PGD_2 production assays
HEK293 cells were plated in 24-well plates and transiently transfected with the indicated constructs. The cells were then incubated for 15 min at 37°C in the presence of 5 µM PGH_2. Secreted PGD_2 present in the media was then measured with the PGD_2 enzyme immunoassay (EIA) kit according to the manufacturer's instructions (Cayman Chemical Co.). GST–L-PGDS and GST–L-PGDS–W43A/G47A were diluted in EIA buffer from the PGD_2 EIA kit. PGH_2 to a final concentration of 0.5 µM was added, and the reaction was performed for 1 min and then stopped with 0.4 mg/ml $SnCl_2$. The PGD_2 produced was then measured with the PGD_2 EIA kit according to the manufacturer's instructions.

Statistical analysis
Statistical analysis was performed using Prism v5.0 (GraphPad Software) using a two-tailed Student's *t* test.

Online supplemental material
Fig. S1 describes the specificity of the L-PGDS interaction with DP1 as HA-tagged L-PGDS coimmunoprecipitates with DP1 but not with other GPCRs tested that included CRTH2, β_2AR, TP-β, and V2R in HEK293 cells. Online supplemental material is available at http://www.jcb.org/cgi/content/full/jcb.201304015/DC1.

The authors wish to thank Dr. Michel Bouvier for providing the V2R and V2R mutant constructs, Dr. Y. Matsuura for Hsp90 constructs, and Terence E. Hebert for helpful suggestions. The authors would also like to thank Dr. Leonid Volkov of the confocal microscopy platform of the Centre de Recherche Clinique Etienne-Lebel for his precious help.

This study was supported by a grant from the Canadian Institutes of Health Research to J.-L. Parent and by the André-Lussier Research Chair.

The authors declare no competing financial interests.

Submitted: 2 April 2013
Accepted: 12 December 2013

References

Belmonte, S.L., and B.C. Blaxall. 2011. G protein coupled receptor kinases as therapeutic targets in cardiovascular disease. *Circ. Res.* 109:309–319. http://dx.doi.org/10.1161/CIRCRESAHA.110.231233

Brinker, A., C. Scheufler, F. Von Der Mulbe, B. Fleckenstein, C. Herrmann, G. Jung, I. Moarefi, and F.U. Hartl. 2002. Ligand discrimination by TPR domains. Relevance and selectivity of EEVD-recognition in Hsp70 · Hop · Hsp90 complexes. *J. Biol. Chem.* 277:19265–19275. http://dx.doi.org/10.1074/jbc.M109002200

Cartier, A., A. Parent, P. Labrecque, G. Laroche, and J.L. Parent. 2011. WDR36 acts as a scaffold protein tethering a G-protein-coupled receptor, Gαq and phospholipase Cβ in a signalling complex. *J. Cell Sci.* 124:3292–3304. http://dx.doi.org/10.1242/jcs.085795

Chen, C.Y., and W.E. Balch. 2006. The Hsp90 chaperone complex regulates GDI-dependent Rab recycling. *Mol. Biol. Cell.* 17:3494–3507. http://dx.doi.org/10.1091/mbc.E05-12-1096

Chiba, T., S. Ueki, W. Ito, H. Kato, R. Kamada, M. Takeda, H. Kayaba, M. Furue, and J. Chihara. 2011. The opposing role of two prostaglandin D2 receptors, DP and CRTH2, in human eosinophil migration. *Ann. Allergy Asthma Immunol.* 106:511–517. http://dx.doi.org/10.1016/j.anai.2011.01.027

Cliff, M.J., R. Harris, D. Barford, J.E. Ladbury, and M.A. Williams. 2006. Conformational diversity in the TPR domain-mediated interaction of protein phosphatase 5 with Hsp90. *Structure*. 14:415–426. http://dx.doi.org/10.1016/j.str.2005.12.009

Conn, P.M., A. Ulloa-Aguirre, J. Ito, and J.A. Janovick. 2007. G protein-coupled receptor trafficking in health and disease: lessons learned to prepare for therapeutic mutant rescue in vivo. *Pharmacol. Rev.* 59:225–250. http://dx.doi.org/10.1124/pr.59.3.2

Décaillot, F.M., R. Rozenfeld, A. Gupta, and L.A. Devi. 2008. Cell surface targeting of mu-delta opioid receptor heterodimers by RTP4. *Proc. Natl. Acad. Sci. USA*. 105:16045–16050. http://dx.doi.org/10.1073/pnas.0804106105

Durand, M., M.A. Gallant, and A.J. de Brum-Fernandes. 2008. Prostaglandin D2 receptors control osteoclastogenesis and the activity of human osteoclasts. *J. Bone Miner. Res.* 23:1097–1105. http://dx.doi.org/10.1359/jbmr.080228

Filipeanu, C.M., R. de Vries, A.H. Danser, and D.R. Kapusta. 2011. Modulation of α(2C) adrenergic receptor temperature-sensitive trafficking by HSP90. *Biochim. Biophys. Acta.* 1813:346–357. http://dx.doi.org/10.1016/j.bbamcr.2010.11.020

Fujimori, K., Y. Kanaoka, Y. Sakaguchi, and Y. Urade. 2000. Transcriptional activation of the human hematopoietic prostaglandin D synthase gene in megakaryoblastic cells. Roles of the oct-1 element in the 5′-flanking region and the AP-2 element in the untranslated exon 1. *J. Biol. Chem.* 275:40511–40516. http://dx.doi.org/10.1074/jbc.M007688200

Gallant, M.A., R. Samadfam, J.A. Hackett, J. Antoniou, J.L. Parent, and A.J. de Brum-Fernandes. 2005. Production of prostaglandin D(2) by human osteoblasts and modulation of osteoprotegerin, RANKL, and cellular

migration by DP and CRTH2 receptors. *J. Bone Miner. Res.* 20:672–681. http://dx.doi.org/10.1359/JBMR.041211

Gallant, M.A., D. Slipetz, E. Hamelin, M.D. Rochdi, S. Talbot, A.J. de Brum-Fernandes, and J.L. Parent. 2007. Differential regulation of the signaling and trafficking of the two prostaglandin D2 receptors, prostanoid DP receptor and CRTH2. *Eur. J. Pharmacol.* 557:115–123. http://dx.doi.org/10.1016/j.ejphar.2006.11.058

García-Cardeña, G., R. Fan, V. Shah, R. Sorrentino, G. Cirino, A. Papapetropoulos, and W.C. Sessa. 1998. Dynamic activation of endothelial nitric oxide synthase by Hsp90. *Nature*. 392:821–824. http://dx.doi.org/10.1038/33934

Gazda, L., W. Pokrzywa, D. Hellerschmied, T. Löwe, I. Forné, F. Mueller-Planitz, T. Hoppe, and T. Clausen. 2013. The myosin chaperone UNC-45 is organized in tandem modules to support myofilament formation in *C. elegans*. *Cell*. 152:183–195. http://dx.doi.org/10.1016/j.cell.2012.12.025

Gorska, M., U. Popowska, A. Sielicka-Dudzin, A. Kuban-Jankowska, W. Sawczuk, N. Knap, G. Cicero, and F. Wozniak. 2012. Geldanamycin and its derivatives as Hsp90 inhibitors. *Front Biosci (Landmark Ed)*. 17:2269–2277. http://dx.doi.org/10.2741/4050

Hartl, F.U., A. Bracher, and M. Hayer-Hartl. 2011. Molecular chaperones in protein folding and proteostasis. *Nature*. 475:324–332. http://dx.doi.org/10.1038/nature10317

He, F., Z.H. Qiao, J. Cai, W. Pierce, D.C. He, and Z.H. Song. 2007. Involvement of the 90-kDa heat shock protein (Hsp-90) in CB2 cannabinoid receptor-mediated cell migration: a new role of Hsp-90 in migration signaling of a G protein-coupled receptor. *Mol. Pharmacol.* 72:1289–1300. http://dx.doi.org/10.1124/mol.107.036566

Hirata, T., and S. Narumiya. 2012. Prostanoids as regulators of innate and adaptive immunity. *Adv. Immunol.* 116:143–174. http://dx.doi.org/10.1016/B978-0-12-394300-2.00005-3

Hohwy, M., L. Spadola, B. Lundquist, P. Hawtin, J. Dahmén, I. Groth-Clausen, E. Nilsson, S. Persdotter, K. von Wachenfeldt, R.H. Folmer, and K. Edman. 2008. Novel prostaglandin D synthase inhibitors generated by fragment-based drug design. *J. Med. Chem.* 51:2178–2186. http://dx.doi.org/10.1021/jm701509k

Imai, J., H. Yashiroda, M. Maruya, I. Yahara, and K. Tanaka. 2003. Proteasomes and molecular chaperones: cellular machinery responsible for folding and destruction of unfolded proteins. *Cell Cycle*. 2:584–590. http://dx.doi.org/10.4161/cc.2.6.586

Jackson, S.E. 2013. Hsp90: structure and function. *Top. Curr. Chem.* 328:155–240. http://dx.doi.org/10.1007/128_2012_356

Kanekiyo, T., T. Ban, K. Aritake, Z.L. Huang, W.M. Qu, I. Okazaki, I. Mohri, S. Murayama, K. Ozono, M. Taniike, et al. 2007. Lipocalin-type prostaglandin D synthase/beta-trace is a major amyloid beta-chaperone in human cerebrospinal fluid. *Proc. Natl. Acad. Sci. USA*. 104:6412–6417. http://dx.doi.org/10.1073/pnas.0701585104

Kriegenburg, F., L. Ellgaard, and R. Hartmann-Petersen. 2012. Molecular chaperones in targeting misfolded proteins for ubiquitin-dependent degradation. *FEBS J.* 279:532–542. http://dx.doi.org/10.1111/j.1742-4658.2011.08456.x

Kumasaka, T., K. Aritake, H. Ago, D. Irikura, T. Tsurumura, M. Yamamoto, M. Miyano, Y. Urade, and O. Hayaishi. 2009. Structural basis of the catalytic mechanism operating in open-closed conformers of lipocalin type prostaglandin D synthase. *J. Biol. Chem.* 284:22344–22352. http://dx.doi.org/10.1074/jbc.M109.018341

Labrecque, P., S.J. Roy, L. Fréchette, C. Iorio-Morin, M.A. Gallant, and J.L. Parent. 2013. Inverse agonist and pharmacochaperone properties of MK-0524 on the prostanoid DP1 receptor. *PLoS ONE*. 8:e65767. http://dx.doi.org/10.1371/journal.pone.0065767

Lachance, V., A. Cartier, S. Génier, S. Munger, P. Germain, P. Labrecque, and J.L. Parent. 2011. Regulation of β2-adrenergic receptor maturation and anterograde trafficking by an interaction with Rab geranylgeranyltransferase: modulation of Rab geranylgeranylation by the receptor. *J. Biol. Chem.* 286:40802–40813. http://dx.doi.org/10.1074/jbc.M111.267815

Lappano, R., and M. Maggiolini. 2012. GPCRs and cancer. *Acta Pharmacol. Sin.* 33:351–362. http://dx.doi.org/10.1038/aps.2011.183

Lebon, G., and C.G. Tate. 2012. G protein-coupled receptors in the spotlight. [In French.] *Med. Sci. (Paris)*. 28:876–882. http://dx.doi.org/10.1051/medsci/20122810017

Leskelä, T.T., P.M. Markkanen, E.M. Pietilä, J.T. Tuusa, and U.E. Petäjä-Repo. 2007. Opioid receptor pharmacological chaperones act by binding and stabilizing newly synthesized receptors in the endoplasmic reticulum. *J. Biol. Chem.* 282:23171–23183. http://dx.doi.org/10.1074/jbc.M610896200

Luo, J., and J.L. Benovic. 2003. G protein-coupled receptor kinase interaction with Hsp90 mediates kinase maturation. *J. Biol. Chem.* 278:50908–50914. http://dx.doi.org/10.1074/jbc.M307637200

Magalhaes, A.C., H. Dunn, and S.S. Ferguson. 2012. Regulation of GPCR activity, trafficking and localization by GPCR-interacting proteins. *Br. J. Pharmacol.* 165:1717–1736. http://dx.doi.org/10.1111/j.1476-5381.2011.01552.x

Mathurin, K., M.A. Gallant, P. Germain, H. Allard-Chamard, J. Brisson, C. Iorio-Morin, A. de Brum Fernandes, M.G. Caron, S.A. Laporte, and J.L. Parent. 2011. An interaction between L-prostaglandin D synthase and arrestin increases PGD2 production. *J. Biol. Chem.* 286:2696–2706. http://dx.doi.org/10.1074/jbc.M110.178277

McClellan, A.J., Y. Xia, A.M. Deutschbauer, R.W. Davis, M. Gerstein, and J. Frydman. 2007. Diverse cellular functions of the Hsp90 molecular chaperone uncovered using systems approaches. *Cell*. 131:121–135. http://dx.doi.org/10.1016/j.cell.2007.07.036

Miyamoto, Y., S. Nishimura, K. Inoue, S. Shimamoto, T. Yoshida, A. Fukuhara, M. Yamada, Y. Urade, N. Yagi, T. Ohkubo, and T. Inui. 2010. Structural analysis of lipocalin-type prostaglandin D synthase complexed with biliverdin by small-angle X-ray scattering and multi-dimensional NMR. *J. Struct. Biol.* 169:209–218. http://dx.doi.org/10.1016/j.jsb.2009.10.005

Morita, I., M. Schindler, M.K. Regier, J.C. Otto, T. Hori, D.L. DeWitt, and W.L. Smith. 1995. Different intracellular locations for prostaglandin endoperoxide H synthase-1 and -2. *J. Biol. Chem.* 270:10902–10908. http://dx.doi.org/10.1074/jbc.270.18.10902

Narumiya, S., Y. Sugimoto, and F. Ushikubi. 1999. Prostanoid receptors: structures, properties, and functions. *Physiol. Rev.* 79:1193–1226.

Oguma, T., K. Asano, and A. Ishizaka. 2008. Role of prostaglandin D(2) and its receptors in the pathophysiology of asthma. *Allergol. Int.* 57:307–312. http://dx.doi.org/10.2332/allergolint.08-RAI-0033

Oksche, A., R. Schülein, C. Rutz, U. Liebenhoff, J. Dickson, H. Müller, M. Birnbaumer, and W. Rosenthal. 1996. Vasopressin V2 receptor mutants that cause X-linked nephrogenic diabetes insipidus: analysis of expression, processing, and function. *Mol. Pharmacol.* 50:820–828.

Pai, K.S., V.B. Mahajan, A. Lau, and D.D. Cunningham. 2001. Thrombin receptor signaling to cytoskeleton requires Hsp90. *J. Biol. Chem.* 276:32642–32647. http://dx.doi.org/10.1074/jbc.M104212200

Parent, A., E. Hamelin, P. Germain, and J.L. Parent. 2009. Rab11 regulates the recycling of the beta2-adrenergic receptor through a direct interaction. *Biochem. J.* 418:163–172. http://dx.doi.org/10.1042/BJ20080867

Parent, A., S.J. Roy, C. Iorio-Morin, M.C. Lépine, P. Labrecque, M.A. Gallant, D. Slipetz, and J.L. Parent. 2010. ANKRD13C acts as a molecular chaperone for G protein-coupled receptors. *J. Biol. Chem.* 285:40838–40851. http://dx.doi.org/10.1074/jbc.M110.142257

Petäjä-Repo, U.E., M. Hogue, S. Bhalla, A. Laperrière, J.P. Morello, and M. Bouvier. 2002. Ligands act as pharmacological chaperones and increase the efficiency of delta opioid receptor maturation. *EMBO J.* 21:1628–1637. http://dx.doi.org/10.1093/emboj/21.7.1628

Rodrigo-Brenni, M.C., and R.S. Hegde. 2012. Design principles of protein biosynthesis-coupled quality control. *Dev. Cell*. 23:896–907. http://dx.doi.org/10.1016/j.devcel.2012.10.012

Rosenbaum, E.E., K.S. Brehm, E. Vasiljevic, C.H. Liu, R.C. Hardie, and N.J. Colley. 2011. XPORT-dependent transport of TRP and rhodopsin. *Neuron*. 72:602–615. http://dx.doi.org/10.1016/j.neuron.2011.09.016

Roy, S.J., I. Glazkova, L. Fréchette, C. Iorio-Morin, C. Binda, D. Pétrin, P. Trieu, M. Robitaille, S. Angers, T.E. Hébert, and J.L. Parent. 2013. Novel, gel-free proteomics approach identifies RNF5 and JAMP as modulators of GPCR stability. *Mol. Endocrinol.* 27:1245–1266. http://dx.doi.org/10.1210/me.2013-1091

Sakisaka, T., T. Meerlo, J. Matteson, H. Plutner, and W.E. Balch. 2002. Rab-alphaGDI activity is regulated by a Hsp90 chaperone complex. *EMBO J.* 21:6125–6135. http://dx.doi.org/10.1093/emboj/cdf603

Scheufler, C., A. Brinker, G. Bourenkov, S. Pegoraro, L. Moroder, H. Bartunik, F.U. Hartl, and I. Moarefi. 2000. Structure of TPR domain-peptide complexes: critical elements in the assembly of the Hsp70-Hsp90 multichaperone machine. *Cell*. 101:199–210. http://dx.doi.org/10.1016/S0092-8674(00)80830-2

Schuligoi, R., E. Sturm, P. Luschnig, V. Konya, S. Philipose, M. Sedej, M. Waldhoer, B.A. Peskar, and A. Heinemann. 2010. CRTH2 and D-type prostanoid receptor antagonists as novel therapeutic agents for inflammatory diseases. *Pharmacology*. 85:372–382. http://dx.doi.org/10.1159/000313836

Sikorski, R.S., M.S. Boguski, M. Goebl, and P. Hieter. 1990. A repeating amino acid motif in CDC23 defines a family of proteins and a new relationship among genes required for mitosis and RNA synthesis. *Cell*. 60:307–317. http://dx.doi.org/10.1016/0092-8674(90)90745-Z

Tadevosyan, A., G. Vaniotis, B.G. Allen, T.E. Hébert, and S. Nattel. 2012. G protein-coupled receptor signalling in the cardiac nuclear membrane: evidence and possible roles in physiological and pathophysiological function. *J. Physiol.* 590:1313–1330.

Taipale, M., D.F. Jarosz, and S. Lindquist. 2010. HSP90 at the hub of protein homeostasis: emerging mechanistic insights. *Nat. Rev. Mol. Cell Biol.* 11:515–528. http://dx.doi.org/10.1038/nrm2918

Tanaka, K., K. Ogawa, K. Sugamura, M. Nakamura, S. Takano, and K. Nagata. 2000. Cutting edge: differential production of prostaglandin D2 by human helper T cell subsets. *J. Immunol.* 164:2277–2280.

Ulloa-Aguirre, A., and P. Michael Conn. 2011. Pharmacoperones: a new therapeutic approach for diseases caused by misfolded G protein-coupled receptors. *Recent Pat. Endocr. Metab, Immune Drug Discov.* 5:13–24. http://dx.doi.org/10.2174/187221411794351851

Urade, Y., and O. Hayaishi. 2000. Biochemical, structural, genetic, physiological, and pathophysiological features of lipocalin-type prostaglandin D synthase. *Biochim. Biophys. Acta*. 1482:259–271. http://dx.doi.org/10.1016/S0167-4838(00)00161-8

Urade, Y., M. Ujihara, Y. Horiguchi, M. Igarashi, A. Nagata, K. Ikai, and O. Hayaishi. 1990. Mast cells contain spleen-type prostaglandin D synthetase. *J. Biol. Chem.* 265:371–375.

Vaniotis, G., B.G. Allen, and T.E. Hébert. 2011. Nuclear GPCRs in cardiomyocytes: an insider's view of β-adrenergic receptor signaling. *Am. J. Physiol. Heart Circ. Physiol.* 301:H1754–H1764. http://dx.doi.org/10.1152/ajpheart.00657.2011

Vassart, G., and S. Costagliola. 2011. G protein-coupled receptors: mutations and endocrine diseases. *Nat. Rev. Endocrinol.* 7:362–372. http://dx.doi.org/10.1038/nrendo.2011.20

Wang, X., J.S. Pattison, and H. Su. 2013. Posttranslational modification and quality control. *Circ. Res.* 112:367–381. http://dx.doi.org/10.1161/CIRCRESAHA.112.268706

Wu, B., P. Li, Y. Liu, Z. Lou, Y. Ding, C. Shu, S. Ye, M. Bartlam, B. Shen, and Z. Rao. 2004. 3D structure of human FK506-binding protein 52: implications for the assembly of the glucocorticoid receptor/Hsp90/immunophilin heterocomplex. *Proc. Natl. Acad. Sci. USA*. 101:8348–8353. http://dx.doi.org/10.1073/pnas.0305969101

Zhao, R., and W.A. Houry. 2007. Molecular interaction network of the Hsp90 chaperone system. *Adv. Exp. Med. Biol.* 594:27–36. http://dx.doi.org/10.1007/978-0-387-39975-1_3

Zhou, Y., N. Shaw, Y. Li, Y. Zhao, R. Zhang, and Z.J. Liu. 2010. Structure-function analysis of human l-prostaglandin D synthase bound with fatty acid molecules. *FASEB J.* 24:4668–4677. http://dx.doi.org/10.1096/fj.10-164863

Zhu, T., F. Gobeil, A. Vazquez-Tello, M. Leduc, L. Rihakova, M. Bossolasco, G. Bkaily, K. Peri, D.R. Varma, R. Orvoine, and S. Chemtob. 2006. Intracrine signaling through lipid mediators and their cognate nuclear G-protein-coupled receptors: a paradigm based on PGE2, PAF, and LPA1 receptors. *Can. J. Physiol. Pharmacol.* 84:377–391. http://dx.doi.org/10.1139/y05-147

Zuiderweg, E.R., E.B. Bertelsen, A. Rousaki, M.P. Mayer, J.E. Gestwicki, and A. Ahmad. 2013. Allostery in the Hsp70 chaperone proteins. *Top. Curr. Chem.* 328:99–153. http://dx.doi.org/10.1007/128_2012_323